

Lectures on renormalization and asymptotic safety

Sandor Nagy

*Department of Theoretical Physics, University of Debrecen, P.O. Box 5, H-4010 Debrecen, Hungary and
MTA-DE Particle Physics Research Group, P.O.Box 51, H-4001 Debrecen, Hungary*

A short introduction is given on the functional renormalization group method, putting emphasis on its nonperturbative aspects. The method enables to find nontrivial fixed points in quantum field theoretic models which make them free from divergences and leads to the concept of asymptotic safety. It can be considered as a generalization of the asymptotic freedom which plays a key role in the perturbative renormalization. We summarize and give a short discussion of some important models, which are asymptotically safe such as the Gross-Neveu model, the nonlinear σ model, the sine-Gordon model, and the model of quantum Einstein gravity. We also give a detailed analysis of infrared behavior of the models where a spontaneous symmetry breaking takes place. The deep infrared behavior of the broken phase cannot be treated within the framework of perturbative calculations. We demonstrate that there exists an infrared fixed point in the broken phase which creates a new scaling regime there, however its structure is hidden by the singularity of the renormalization group equations. The phase spaces of these models show several similar properties, namely the models has the same phase and fixed point structure. These results can only be uncovered by the functional renormalization group method.

PACS numbers: 11.10.Gh, 11.10.Hi, 04.60.-m

Keywords: functional renormalization group, asymptotic safety, infrared fixed point

I. INTRODUCTION

The concept of asymptotic safety can be understood in the framework of quantum field theory, where we treat quantum systems with many degrees of freedom and many orders of magnitude in length, or in energy, momentum. Usually we have an assumption of describing the high energy/ultra violet (UV), or short distance/microscopic interactions among the elementary particles where a high degree of symmetry exists. However the measurements are typically performed at low energies, in the infrared (IR) regime, therefore we need the theory, where those quantum fluctuations or modes are taken into account which energy is between the UV and IR energy scales. The functional renormalization group (RG) method is one of the best candidate to take into account the quantum fluctuations step by step, one by one, systematically [1–7]. The method provides us a partial differential equations for the action of the model. As an initial condition we need the UV action, and the solution of the equation gives us the IR one which can be identified with the effective potential. If these scales are close to each other, then even a perturbative treatment can be satisfactory. However, generally one cannot conclude to the IR behavior from the UV one.

The effective action can be derived from the blocked action. We assume (especially in scalar models), that the blocked and the effective action has the same functional structure. We usually perform a field expansion to the effective action which results in many interacting terms, and each of them is multiplied by a coupling. The original partial differential equation can be converted to a system of ordinary differential equations w.r.t. the couplings. These equations are called evolution or flow equations. The initial conditions are the UV values of the couplings and the results of the equations are the IR ones. The RG method typically gives highly nonlinear evolution equations, giving flows which cannot be recovered by a perturbative RG treatment.

Moreover the perturbative RG calculations are performed in the vicinity of the Gaussian fixed point (GFP). The GFP is the origin of the phase space which is spanned by the (dimensionless) couplings. The UV effective action is given by small values of the initial couplings, so the kinetic term dominates the UV physics. The UV scaling of the couplings are UV attractive or IR repulsive (they go away from the fixed point if we consider the direction of the RG 'time' scale) if the model is perturbatively renormalizable. Otherwise it may happen that the GFP is a hyperbolic point which means that there are directions in the phase space which are UV attracted by the GFP but there are certain ones which are UV repulsed. In the latter case the perturbative flow equations give that the corresponding couplings go to infinity, which seems nonphysical. However the model can be safe from divergences if besides the GFP there exists a further nontrivial fixed point in the finite region of the phase space which UV attracts the trajectories, as the GFP does in the perturbatively renormalizable case. It can make the physical quantities finite, due to the finiteness of the dimensionless couplings. The nontrivial fixed point is usually referred to as a non Gaussian fixed point (NGFP). This is the main idea of asymptotic safety, Shortly, it means that there exists an UV attractive NGFP in the phase space.

The paper is organized as follows. In Sect. II we give a short introduction on the functional RG method with some basic concepts and tools. Then the d -dimensional $O(N)$ model is investigated as a classical example of the asymptotic

freedom. In Sect. III we treat the asymptotic safety, as the generalization of the idea of the asymptotic freedom. It is shown in the framework of the nonlinear σ , Gross-Neveu, sine Gordon and quantum Einstein gravity models how the asymptotic safety takes place. In Sect. IV the conclusions are drawn up.

II. RENORMALIZATION

The functional renormalization group method is one of the most useful nonperturbative tool to investigate quantum field theoretic models. We define a model by its action at a high (UV) energy scale, because at UV the form of the action is generally quite simple due to the high symmetries appearing at large energies, which belongs to the short distance microscopic interactions. The UV action contains interaction terms multiplied by the UV couplings. The RG method systematically eliminates the degrees of freedom of the theory in order of decreasing energy, and provides us the value of the couplings at lower energy scales. As a result we obtain the value of IR couplings at practically zero energies. The IR the effective potential usually has an involved structure. There the long-range interactions may induce further couplings and can induce non-localities, or global condensates.

The nonperturbative nature of the functional RG can be nicely enlightened, if one considers the tunneling, which is a highly nonperturbative phenomenon in Quantum Mechanics. In the path integral formulation of QFT the extremum of the UV action is the classical path. Thus if one treats QM then the tree level RG evolution corresponds to this classical path. It implies that the RG method should dress up the couplings in such a way which can drive the classical path to a path which corresponds to the tunneling process. Naturally it requires all the modes till the deep IR regime [8–12]. Moreover we need further terms in the gradient expansion. We note that the tunneling can be treated by a more exact manner in the framework of solving Schrodinger equation with the corresponding potential numerically. However the Schrodinger equation can be considered as an effective theory, while the path integral formulation of QFT is more fundamental. The wavefunction which corresponds to the tunneling should be combined from practically plane waves since the field variables in QFT are expanded from them. If one includes higher order terms in the derivative expansion then more involved functions can appear in the field expansion. This fact requires to take into account all the modes and the wavefunction renormalization. Both can be systematically treated in the framework of the RG method.

The quantized anharmonic oscillator coupled to a heat bath provides us a system, where the “holy grail” of the phase transitions, namely the quantum-classical transition can be investigated [13–18]. The heat bath can be considered as the environment of the original quantized oscillator, which can be identified by the system. The environment can be represented by harmonic oscillators which are coupled to the system. The RG procedure integrates out the environment and leads to an effective system. It appears as if the quantum effects are dissipated by the environment driving the system to a classical regime.

The RG method can be used in a powerful manner in almost every area of modern physics. In condensed matter systems, e.g. one can investigate the Bose-Einstein condensate – BCS superconductor transition for ultracold fermionic atoms [19–21]. Furthermore the RG method can account for the essential scaling of the correlation length, which typically appears in low dimensional thin superfluid film structures. The appearing Kosterlitz-Thouless (KT) type or infinite order phase transitions [22, 23] can be described in the framework of the 2d $O(2)$ model [24, 25], in the 2d sine-Gordon (SG) model, too [26–29], or its generalization in fermionic models [30, 31].

New ideas or improvements of the RG method are usually investigated in the d -dimensional $O(N)$ model. The calculation of the critical exponents in the 3d $O(N)$ model provides us a widely acceptable testing ground of the functional renormalization. One can get the exponents by field expansion of the potential [32–34], or by ϵ -expansion in $4 - \epsilon$ dimensions [35–37]. The convergence of the exponents in the derivative expansion is also investigated [38–42], however preciser results can be obtained without expanding the potential [43–45]. Furthermore, the supersymmetric version of the model has also been attracted a considerable attention [46, 47]. The exponents can be determined from IR scalings, too [48]. Likewise, less computational effort can give very good results for the exponents by using the BMW approximation, where the full momentum dependence of the correlation functions is considered [49–51].

The RG treatment of 2+1 fermionic systems has a revival since the new results on graphene. The Gross-Neveu model [52–54] give on the other hand a good testing ground to investigate a model with NGFP and asymptotic safety. The Thirring model [55, 56] serves as a good playing ground to investigate the chiral symmetry breaking, which appears in electroweak interactions. The nonperturbative treatment of the RG method is capable of describing quantum electrodynamics [57–59], non-abelian gauge theories [60–67], furthermore the confining mechanism in quantum chromodynamics even in finite temperature and chemical potential [68–71].

The nonlinear σ model itself has a widebroad interest in many branches in quantum physics starting from phenomenological aspects of high energy physics, condensed matter systems, and strings. Furthermore it exhibits a symmetric and a broken symmetric phase, similarly to the $O(N)$ model and the quantum Einstein gravity (QEG), and the model also has a NGFP in the UV [72–76]. The other common feature with QEG is that they have nonpoly-

nomial interactions, the couplings have the same dimension there, and both models need background field technique to construct the RG equations [74] which is widely used in gauge theories [77] and in QEG [78]. Among the low dimensional scalar models we also mention the 2d SG model [79], which is non-trivial quantum field theory with compact variables – similarly to the non-Abelian gauge theories – which is supposed to be the key to the confinement mechanism. The functional RG treatment shows that the SG model has two phases [28, 29, 80, 81] and there is an IR fixed point in the broken phase [28, 29], furthermore the model has both an UV Gaussian and a NGFP, and what is more, the latter shows singularity.

The IR limit of the RG flows is also a great challenge to reach. In scalar models the IR scaling of the symmetric phase can be easily obtained. It can be characterized by such an effective potential that has a well defined single minimum at the origin at the value of the field variable $\phi = 0$. In the phase with spontaneously broken symmetry the effective potential tends to be degenerate which means that a plateau starts to form in the potential around the origin [2, 6, 82]. It is due to the huge amount of soft (nearly zero energy) modes which can excite the ground state without energy practically [3, 83, 84]. In this region of the phase space the perturbative treatments naturally do not work. However the RG method uncovers us that there is an IR fixed point in the broken phase [28–30, 82, 85]. One can define the correlation length in the IR regime which can help us to determine the corresponding critical exponent ν , moreover one can also determine the order of the phase transition of the model [48, 86, 87]. The IR fixed point explicitly shows the limitation of the theory where it can be treated by its original degrees of freedom. The bulk amount of soft modes show that new elementary excitations arise in the model at low energies and its treatment needs a new model, or at least some new interaction terms.

The other limit towards the UV gives a further challenge of the RG method. Recently the UV limit of QEG is widely investigated [78, 88–93]. The model usually has a GFP. However around the GFP the Newton constant or coupling starts to blow up in the UV limit, which makes the physical quantities infinitely large there. It implies that the model is perturbatively nonrenormalizable [94, 95]. As a possible solution for this problem it was conjectured [96–99] and later showed in low dimensions [100, 101], that there is a further UV NGFP fixed point in the phase space which makes the Newton constant finite and the model becomes safe from divergences, which is called asymptotic safety [91, 102–105]. Interestingly the model also has an IR fixed point in its broken phase [87, 106–110].

A. Blocking

QFT can be formulated by using the path integral formalism [111]. The generating functional expresses the vacuum-vacuum transition amplitude and has the form

$$Z = \int \mathcal{D}\phi e^{-S_k} = \int d\phi_0 \dots d\phi_{k-\Delta k} d\phi_k d\phi_{k+\Delta k} \dots d\phi_\infty e^{-S_k} \quad (1)$$

where S_k is the (blocked) action at the momentum scale k . The extremum of the action gives the classical path. The path integral is performed for all the possible paths between the given initial and final states. In order to handle them we order the paths according to e.g. by their momentum [112] or even by their amplitude in the internal space [113]. The procedure leads to the Wetterich equation [1] for the effective average action [114]. We can assign a certain k to each path, usually we enumerate them by their decreasing value. We note that the momentum k is basically a bookkeeping device for the modes, and it has no direct connection to any value of energy or momentum of the modes. The RG method provides us a systematic treatment to take into account the quantum fluctuation systematically. The modes are integrated out one by one in with decreasing value of k . After the elimination of some modes, the action changes to $S_{k-\Delta k}$, which is given at the lower scale $k - \Delta k$. If one eliminates the modes in the vicinity of the UV scale, then we recover the perturbative RG treatment.

The highest scale k is the UV cutoff, which is denoted by k_Λ . The blocked action is built up on e.g. symmetry considerations or analogies to other field theoretic models. Usually the action contains a kinetic and a potential terms, the latter contains interacting terms that are multiplied by couplings, and they carry the scale dependence in the action. The couplings usually have physical meaning, they can be related to e.g. particle masses or interaction couplings. The initial value of the couplings should be given at a high energy UV scale describing short-range interactions. If one integrates out the modes between the scales k and $k - \Delta k$ then the value of the coupling changes. It is illustrated in Fig. 1, where the coupling is denoted by g_k .

The figure illustrates how the value of the coupling changes as the scale k decreases. The scale k starts at k_Λ and tends to zero. One has to integrate out infinitely many degrees of freedom, where the modes are enumerated by the continuous index k . The coupling becomes a scale dependent function, the RG evolution eventually gives how the

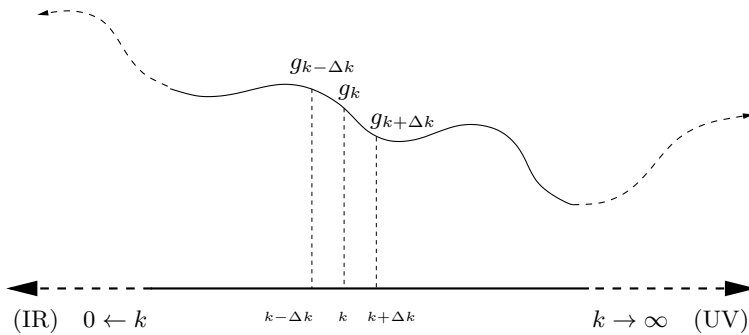


FIG. 1: The change of the coupling g is presented as the scale changes from $k + \Delta k \rightarrow k \rightarrow k - \Delta k$. The limit $k \rightarrow \infty$ ($k \rightarrow 0$) corresponds to the UV (IR) limits, respectively.

value of the coupling changes till we reach the scale $k = 0$, and then we obtain the effective potential which contains the coupling g_0 . From this point of view the functional RG method can be considered as a tool to perform the path integral in the generating functional.

The RG method gives a partial differential equation for the action, however if one takes a functional ansatz for its functional form, e.g.

$$S_k[\phi, g_i] = \sum_i g_i(k) \mathcal{F}_i(\phi), \quad (2)$$

then one can deduce a system of differential equations for the couplings. Here k denotes the scale, $g_i (= g_i(k))$ are the dimensionful couplings, and ϕ is the field variable. The functionals \mathcal{F} is typically Taylor expanded according to its field variable but there are situations where a Fourier expansion is required if one would like keep the periodic symmetry.

B. The Wetterich equation

The RG evolution equation for the blocked action is derived by Wilson [115] and Polchinski [116]. Wilson's idea considers the quantum fluctuation by decreasing order in the scale k , which can correspond to the summation of the loop expansion. There the short distance interactions are integrated out in order to get an effective long distance theory. Polchinski's RG method seems to sum up the perturbative expansion systematically [3].

The Wetterich equation is a functional integro-differential equation for the effective action [1, 2]. We start its derivation from the generating functional

$$Z = e^{W_k[J]} = \int \mathcal{D}[\phi] e^{-(S_k + \mathcal{R}_k[\phi] - J \cdot \phi)}, \quad (3)$$

in Euclidean spacetime, where J denotes the source of the field variable. We use the notation $f \cdot g = \int_{-\infty}^{\infty} d^d x f(x) g(x)$. The integral gives the average of fields over a volume k^{-1} . One integrates out the modes with the scale larger than k . There is an additional term besides the action, which is called the IR regulator, and it has the form

$$\mathcal{R}_k[\phi] = \frac{1}{2} \phi \cdot \mathcal{R}_k \cdot \phi, \quad (4)$$

which acts as an IR cutoff. Here the dots also denote momentum integrals. The IR regulator guarantees that the modes with its scale larger than k are taken into account in an unaltered way while the modes with scale smaller than k are suppressed. It should satisfy the conditions

1. $\lim_{p^2/k^2 \rightarrow 0} \mathcal{R}_k > 0$, i.e. it serves as an IR regulator, since it removes the IR divergences,
2. $\lim_{k^2/p^2 \rightarrow 0} \mathcal{R}_k \rightarrow 0$, which expresses that if the regulator is removed, then we get back Z when $k \rightarrow 0$, so we obtain back the original model in this limit,
3. $\lim_{k^2 \rightarrow \infty} \mathcal{R}_k \rightarrow \infty$, which ensures that the microscopic action can be recovered in the limit $S = \lim_{k \rightarrow \Lambda} \Gamma_k$. It also serves as an UV regulator.

We have many possibilities to choose a functional from to the IR regulator [4, 34, 117–120]. Some typical regulators which are used frequently in the literature are

$$\mathcal{R}_k = ap^2 \frac{e^{-b(p^2/k^2)^c}}{1 - e^{-b(p^2/k^2)^c}} \quad (\text{exponential}), \quad (5)$$

$$\mathcal{R}_k = p^2 \left(\frac{k^2}{p^2} \right)^b \quad (\text{power law}), \quad (6)$$

$$\mathcal{R}_k = (k^2 - p^2)\theta(k^2 - p^2) \quad (\text{optimized or Litim's}). \quad (7)$$

The effective potential should not depend on the IR regulator but due to the truncation of the functional ansatz for the action induces regulator dependence, therefore one has to check how the obtained flows depend on them. Differentiating both sides of Eq. (3) by k one obtains

$$\begin{aligned} \partial_k W_k[J] &= e^{-W_k[J]} \int \mathcal{D}[\phi] \partial_k \mathcal{R}_k e^{-(S_k + \mathcal{R}_k[\phi] - J \cdot \phi)} \\ &= -e^{-W_k[J]} \partial_k \mathcal{R}_k \left[\frac{\delta}{\delta J} \right] e^{W_k[J]}. \end{aligned} \quad (8)$$

The effective action $\Gamma_k[\phi]$ is the Legendre transform of $W_k[J]$, i.e.

$$\Gamma_k[\phi] = -W_k[J] + J \cdot \phi, \quad (9)$$

with the field variable

$$\phi = \frac{\delta W[J]}{\delta J}. \quad (10)$$

The derivative of the effective action $\Gamma_k[\phi]$ w.r.t the scale k is

$$\partial_k \Gamma_k[\phi] = -\partial_k W_k[J] - \frac{\delta W[J]}{\delta J} \partial_k J + \partial_k J \phi = -\partial_k W_k[J]. \quad (11)$$

We redefine the effective action according to $\Gamma_k[\phi] + \mathcal{R}_k[\phi] \rightarrow \Gamma_k$, introduce the 'RG time' $t = \log \frac{k}{k_0}$ and then we obtain the Wetterich equation

$$\dot{\Gamma}_k = \frac{1}{2} \text{Tr} \frac{\dot{\mathcal{R}}_k}{\mathcal{R}_k + \Gamma_k''}, \quad (12)$$

where the notations $' = \partial/\partial\varphi$ and $\dot{} = \partial/\partial t$ are used and the trace Tr stands for the integration over all momenta and the summation over the internal indices. The functional form of the effective action is assumed to be similar to the microscopic action

$$\begin{aligned} \Gamma_k &\sim S_k \\ &= \sum_i g_i(k) \mathcal{F}_i(\phi). \end{aligned} \quad (13)$$

Typically the effective action for scalar fields has the form

$$\Gamma_k = \int d^d x \left[\frac{1}{2} Z_k(\phi_x) (\partial_\mu \phi_x)^2 + V_k(\phi_x) \right], \quad (14)$$

where $Z_k \equiv Z_k(\phi_x) = Z_k(\phi, p)$ is the wavefunction renormalization. It is the next to leading order contribution to the gradient expansion of the action in the field variable after the local potential approximation (LPA). When we use the latter approximation the wavefunction renormalization does not evolve, implying that $Z_k = 1$. Further terms in the derivative expansion can be

$$\Gamma_k = \int d^d x \left[V_k(\phi_x) + \frac{1}{2} Z_k(\phi_x) (\partial_\mu \phi_x)^2 + H_1(\phi_x) (\partial_\mu \phi_x)^4 + H_2(\phi_x) (\square \phi_x)^2 + \dots \right]. \quad (15)$$

If one inserts the form of the effective action in Eq. (14) into Eq. (12), then one obtains the following evolution equation for the potential

$$\dot{V}_k = \frac{1}{2} \int_p \frac{\dot{\mathcal{R}}_k}{Z_k p^2 + \mathcal{R}_k + \tilde{V}_k''}, \quad (16)$$

with the d-dimensional momentum integral. Assuming that the wavefunction renormalization is momentum independent, i.e. $Z_k(\phi, p) = Z_k(\phi) \equiv Z_k$, then one obtains the evolution equation

$$\begin{aligned} \dot{Z}_k = \frac{1}{2} \int_p \dot{\mathcal{R}}_k \left[-\frac{Z_k''}{[p^2 Z_k + \mathcal{R}_k + V_k'']^2} + \frac{\frac{2}{d} Z_k'^2 p^2 + 4 Z_k' (Z_k' p^2 + V_k''')}{(p^2 Z_k + \mathcal{R}_k + V_k'')^3} + \frac{\frac{8}{d} p^2 (Z_k' p^2 + V_k''')^2 (Z_k + \partial_{p^2} \mathcal{R}_k)^2}{(p^2 Z_k + \mathcal{R}_k + V_k'')^5} \right. \\ \left. - 2 \frac{(Z_k' p^2 + V_k''')^2 (Z_k + \partial_{p^2} \mathcal{R}_k + \frac{2}{d} p^2 \partial_{p^2}^2 \mathcal{R}_k) + \frac{4}{d} Z_k' p^2 (Z_k' p^2 + V_k''') (Z_k + \partial_{p^2} \mathcal{R}_k)}{(p^2 Z_k + \mathcal{R}_k + V_k'')^4} \right] \end{aligned} \quad (17)$$

for the wavefunction renormalization.

If one Taylor expands the potential V_k by its field variable, then one arrives at the potential for d-dimensional one component scalar ϕ^4 model of the form

$$V_k = \sum_{n=1}^N \frac{g_{2n}}{(2n)!} \phi^{2n}. \quad (18)$$

After inserting it into Eq. (16) then one obtains a system of ordinary differential equations for the evolution of the couplings. By using the Litim's regulator in Eq. (7) the momentum integral in Eq. (16) can be analytically performed in any dimensions. It is

$$\dot{V}_k = 2v_d k^d \frac{2}{d} \frac{k^2}{k^2 + V''}, \quad (19)$$

where

$$v_d = \frac{1}{2^{d+1} \pi^{d/2} \Gamma(d/2)}, \quad (20)$$

with $\Gamma(d)$ the Gamma function. The form of the evolution equations for the dimensionful couplings is

$$\dot{g}_i = \beta_i(g_j, k), \quad (21)$$

with the β functions. In case of the of the ϕ^4 model their general forms are

$$\beta_i(g_j, k) = \partial_\phi^i \left(\frac{1}{2} \int_p \frac{\dot{\mathcal{R}}_k}{p^2 + \mathcal{R}_k + V_k''} \right) \Big|_{\phi=0}, \quad (22)$$

in LPA, which becomes

$$\beta_i(g_j, k) = \partial_\phi^i \left(2v_d k^d \frac{2}{d} \frac{k^2}{k^2 + V''} \right) \Big|_{\phi=0}, \quad (23)$$

if one uses the Litim's regulator.

C. Evolution equations

One can reformulate the evolution equations in Eq. (21) and the β functions into dimensionless expressions according to

$$\dot{\tilde{g}}_i = -d_i \tilde{g}_i + \alpha_i(\tilde{g}_j) \equiv \tilde{\beta}_i(\tilde{g}_j), \quad (24)$$

where $\alpha_i(\tilde{g}_j) = \beta_i(g_j k^{-d_j}, 1)$. The dimensionless couplings can be related to the dimensionful ones as $\tilde{g}_i = k^{-d_j} g_i$ with d the canonical (mass) dimension.

The evolution equations are usually highly nonlinear system of ordinary differential equations, which have no analytic solutions in general. If the phase space which is spanned by the dimensionless couplings is of high dimension, then it is extremely difficult map out the whole phase structure numerically. Therefore it can be useful to find such a tool which enables us not to avoid the most important parts of the phase space, i.e. where the evolution slows down or even stops. The points where the latter situation takes place are called fixed points. The fixed point of the evolution equations is defined as the singularity or stationary points of the evolution equations, i.e. which satisfies

$$\dot{\tilde{g}}_i = 0. \quad (25)$$

The couplings which are the solutions of the system of algebraic equations in Eq. (25) are denoted by \tilde{g}_i^* . Naturally the fixed points can be usually found only numerically. In the vicinity of the fixed points, due to the slowing down of the RG evolution, the flow equations can be linearized. We note that the linearized flow equations can differ around different fixed points. If we introduce $y_i = \tilde{g}_i - \tilde{g}_i^*$ we obtain the linearized evolution equations

$$\dot{y}_i = M_{ij}y_j, \quad (26)$$

with the matrix

$$M_{ij} = \frac{\partial \tilde{\beta}_i}{\partial \tilde{g}_j}, \quad (27)$$

that can be constructed by taking the derivative of the β functions w.r.t. the dimensionless couplings. The eigenvalues of the matrix M are denoted by s_n . One can diagonalize M , with the help of a linear transformation represented by the matrix S which satisfies the relation $S_{ik}^{-1}M_{kl}S_{ln} = \delta_{in}s_n$. We introduce $z_i = S_{ik}^{-1}y_k$ in order to decouple the linearized flow equations according to

$$\dot{z}_i = s_i z_i. \quad (28)$$

Its solution reads as

$$z_i = z_i(k_\Lambda)e^{s_i t} = z_i(0) \left(\frac{k}{k_\Lambda} \right)^{s_i}, \quad (29)$$

where k_Λ is some reference scale, depending on the fixed point under investigation it can be e.g. the UV cutoff. The real part of the eigenvalue determines whether the trajectory is attracted or repelled by the corresponding fixed point.

D. Classification of fixed points

Let us assume that we have two dimensionless couplings, thus the phase space is 2-dimensional. It is quite straightforward to generalize the classification for higher dimensional phase spaces, although the structure is a bit more complicated. It is clear that the signs of the eigenvalues determine whether we approach or go away from the fixed point where the linearization is performed. In this simple example case the eigenvalues are the solutions of a second order algebraic equation, therefore in general they are complex numbers. The imaginary part of the eigenvalues cannot alter the distance from the fixed point, altogether they make some oscillations around it. Thus the real parts of the eigenvalues determine the types of the scalings of the couplings.

Let us denote the eigenvalues by s_1 and s_2 , and consider the UV limits, i.e. $k \rightarrow \infty$. According to the solution in Eq. (29) we have six possibilities.

1. The eigenvalues are real, $s_1, s_2 \in \mathbb{R}$ and they are negative, $s_1, s_2 < 0$. Then the trajectory approaches the fixed point, and is called an attractive fixed point.
2. $s_1, s_2 \in \mathbb{R}$ and $s_1, s_2 > 0$. Then the trajectory goes away from the fixed point, and it is called a repulsive fixed point.
3. $s_1, s_2 \in \mathbb{R}$ and with opposite signs. Then there is a direction which flows into the fixed point, and there is another one where the flow is repelled by the fixed point. The fixed point is called a hyperbolic point or a saddle point.
4. The eigenvalues are complex $s_1, s_2 \in \mathbb{C}$. They are necessarily constitute complex conjugate pairs. Here the signs of the real parts of the eigenvalues determine how the trajectories behave. If $\Re s_1, \Re s_2 < 0$, then the fixed point attracts the trajectories. The imaginary parts of the eigenvalues give some oscillation for the trajectory. The fixed point is called an attractive focal point.

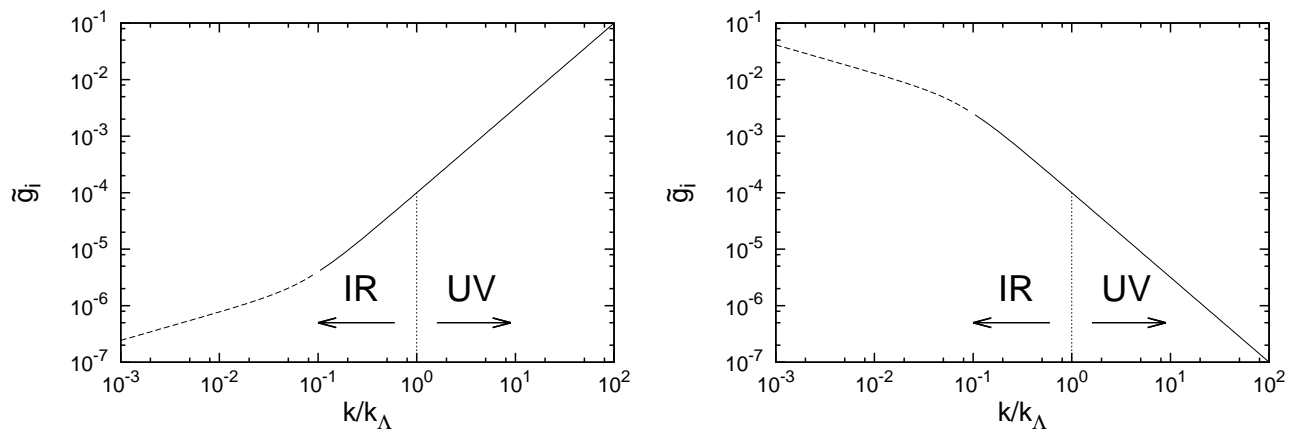


FIG. 2: The irrelevant and relevant scalings of the couplings are shown. In the irrelevant case the the value of the coupling tends to ∞ with a power law behavior as $k \rightarrow \infty$, and the scaling remains unchanged then, since the linearization gives better and better approximation. The value of the couplings decreases when the trajectory goes away from the UV regime. Its power law behavior is limited to the attractive region of the fixed point, far from its scaling regime it can deviate from the power law one. In this example it appears at $k \approx 0.1$. Then a new linear section can appear due to a possible other fixed point in the phase space. Naturally the new fixed point can turn the irrelevant scaling even into a relevant one. In the other figure the relevant scaling is shown. There the $\tilde{g} \rightarrow 0$ as $k \rightarrow \infty$, while it grows up in the opposite direction of the scale.

5. $s_1, s_2 \in \mathbb{C}$ and $\Re s_1, \Re s_2 > 0$. Then the trajectory is repelled by the fixed point, and it is called a repulsive focal point.
6. $s_1, s_2 \in \mathbb{C}$ and the real part is zero. Then, due to the oscillation the trajectory circulates around the fixed point along a closed trajectory. It is called an elliptic point.

Here we assumed that the eigenvalues are nonzero. If one of them is zero, then the other determines, whether the trajectory is attracted or repelled by the fixed point. If both are zero, then one should calculate those terms beyond the linearized approximation in the β functions in Eq. (24), which can give nontrivial contribution. We also note that the classification according to the IR limit $k \rightarrow 0$ using Eq. (29) gives opposite trends for the trajectories.

E. The Gaussian fixed point

The GFP corresponds to the origin of the phase space, i.e. $\tilde{g}_i^* = 0$. It describes a free theory for massless particles. Let us see the linearization of the flow equations in the vicinity of the GFP. If one Taylor expands the β functions around the origin of the phase space then one obtains that

$$\tilde{\beta}_i = -d_i \tilde{g}_i + a_{ij} \tilde{g}_j + a_{ijk} \tilde{g}_j \tilde{g}_k \dots \quad (30)$$

The matrix M defined in Eq. (27) is

$$M_{ij} = -d_{ij} + a_{ij}, \quad (31)$$

but one can prove that $a_{ij} = 0$, when $i < j$, therefore the eigenvalues are simply equal to the negative of the canonical dimensions, i.e.

$$s_i = -d_i. \quad (32)$$

It implies that all the eigenvalues are real in the GFP. The sign of the eigenvalue determines how the coupling behaves as we approach or go away from the GFP. If $s_i > 0$ which means that the canonical dimension is negative $d_i < 0$ then the transformed coupling $z_i \rightarrow \infty$ when the scale $k \rightarrow \infty$ or the RG time $t \rightarrow \infty$, implying that $\tilde{g}_i \rightarrow \infty$ so the trajectory is repelled by the GFP. We illustrate it in Fig. 2. If the scale k is lowered then the coupling tends to zero, and it becomes less and less important as $k \rightarrow 0$, therefore we call the coupling \tilde{g}_i as an irrelevant one. It implies that the irrelevancy is defined according to the IR scaling behavior, and it represents how the flow changes if the

trajectory goes away from the fixed point. Otherwise this definition is meaningful only for the GFP, since it assumes real eigenvalues. Its generalization is however quite straightforward by considering the real parts of the eigenvalues. One cannot conclude from an UV behavior to the IR one, since the trajectory can approach many other fixed points which can totally overwrite its scaling behavior there.

The other possibility is when the eigenvalue of M in Eq. (27) is negative, i.e. $s_i < 0$ giving positive canonical dimension $d_i > 0$. Then $z_i \rightarrow 0$ i.e. $\tilde{g}_i \rightarrow \tilde{g}_i^*$ when k or $t \rightarrow \infty$. In this situation the trajectory is attracted by the GFP, see Fig. 2. The coupling \tilde{g}_i is said to be relevant, since it becomes more and more important as the trajectory goes away from the fixed point. The appearance of a new fixed point besides the GFP can overwrite the scaling properties of the couplings. Furthermore they can save the flows from the singularities [29, 48, 86, 87]. A coupling is said to be marginal if the corresponding eigenvalue is zero. The dimension of the critical surface equals the number of negative eigenvalues.

We call a theory perturbatively renormalizable if $\forall d_i > 0$ in the vicinity of the GFP. In this case we have only renormalizable couplings. A theory is asymptotically free if every value of the coupling tends to zero in the UV limit, i.e. $\lim_{t \rightarrow \infty} \tilde{g}_i = 0$ for $\forall \tilde{g}_i$ around the GFP. Examples for asymptotically free theories are e.g. QCD, and the 3-dimensional ϕ^4 model.

The values of the irrelevant couplings blow up in the UV, and this makes measurable quantities nonphysical, since they will be infinitely large. However one can relate them to critical exponents. If s is the negative eigenvalue of the matrix M , then its negative reciprocal gives the mass critical exponent ν , or the exponent of the correlation length ξ , i.e.

$$\nu = -1/s. \quad (33)$$

Let us recall that the scaling of the correlation length is

$$\xi \sim (T - T_c)^{-\nu}, \quad (34)$$

for continuous or second order phase transitions, where T is the temperature, and T_c is the critical temperature.

F. d-dimensional $O(N)$ model

As an example of asymptotically free theory, we treat the d-dimensional $O(N)$ model by functional RG method. We map out its phase structure, find the fixed points and the corresponding exponents. Although most scalar models are only toy models, but the $O(N)$ model has experimental realization for certain values of N , i.e. they can characterize the following physical systems:

$N = 0$ polymers,

$N = 1$ liquid-vapour transition, or uniaxial (Ising) ferromagnets,

$N = 2$ He^2 superfluid phase transition,

$N = 3$ Heisenberg ferromagnets,

$N = 4$ chiral phase transition for two quark flavors.

The 3d $O(1)$ or 3d ϕ^4 model is a widely investigated model, and it possesses a nontrivial fixed point. Using Eq. (19) for $d = 3$, one can get the following evolution equation for the dimensionful potential

$$\dot{V} = \frac{1}{6\pi^2} \frac{k^5}{k^2 + V''}, \quad (35)$$

if we use the Litim's regulator. If the functional form of the potential in Eq. (18) is inserted to the evolution equation, then one can obtain the β functions for the couplings. Their dimensionless forms are

$$\begin{aligned} \tilde{\beta}_2 &= -2\tilde{g}_2 - \frac{\tilde{g}_4}{8\pi(1 + \tilde{g}_2)^{1/2}}, \\ \tilde{\beta}_4 &= -\tilde{g}_4 + \frac{3\tilde{g}_4^2}{16\pi(1 + \tilde{g}_2)^{3/2}}, \end{aligned} \quad (36)$$

where we neglected the evolution of further couplings which are generated by the RG procedure. In the symmetric phase their effects are really negligible, but they play crucial role in the evolution broken phase. Other regulators

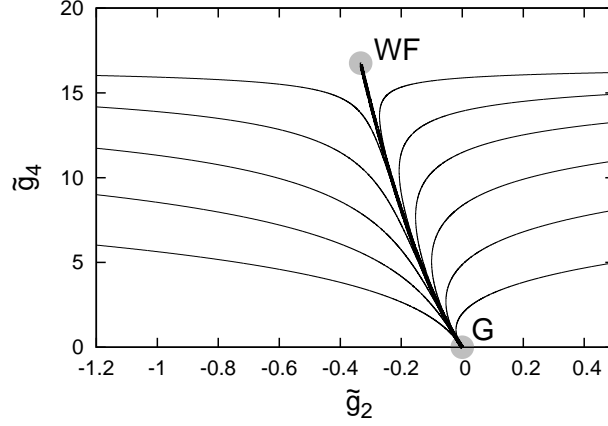


FIG. 3: The phase structure of the 3d ϕ^4 model treated perturbatively. The model has a GFP and a WF fixed point.

would give qualitatively similar equations but e.g. with different multiplication factors, or different exponents in the denominator in the second term on the r.h.s.. Here we do not derive the perturbative RG equations, instead we expand the β functions in Eq. (36) by the coupling \tilde{g}_4 . The zeroth order approximation gives the flows driven by the canonical dimensions. They are

$$\dot{\tilde{g}}_i = \tilde{g}_i(k_\Lambda) e^{-d_i t}, \quad (37)$$

with $g_i(k_\Lambda)$ the initial value and

$$d_i = d + i \left(1 - \frac{d}{2}\right), \quad (38)$$

the canonical dimension of the coupling. This approximation of the flow equations has a GFP. The matrix M in Eq. (27) is

$$M = \begin{pmatrix} \partial_{\tilde{g}_2} \beta_2 & \partial_{\tilde{g}_4} \beta_2 \\ \partial_{\tilde{g}_2} \beta_4 & \partial_{\tilde{g}_4} \beta_4 \end{pmatrix} = \begin{pmatrix} -2 & 0 \\ 0 & -1 \end{pmatrix}, \quad (39)$$

with the eigenvalues $s_1 = -2$ and $s_2 = -1$. Thus the GFP is an UV attractive point, and both couplings are relevant. The eigenvalues and the type of the GFP do not change if one considers further terms in the approximation. Taking into account the next term in the expansion of the flow equations in Eq. (36) one gets

$$\begin{aligned} \dot{\tilde{g}}_2 &= -2\tilde{g}_2 - \frac{\tilde{g}_4}{8\pi} + \mathcal{O}(\tilde{g}_i^2), \\ \dot{\tilde{g}}_4 &= -\tilde{g}_4 + \frac{3\tilde{g}_4^2}{16\pi} + \mathcal{O}(\tilde{g}_i^3). \end{aligned} \quad (40)$$

The structure of the phase space is plotted in Fig. 3. The model has two fixed points. They can be found by solving the system of algebraic equations $\tilde{\beta}_2 = 0$ and $\tilde{\beta}_4 = 0$. The first is the GFP, $\tilde{g}_2^* = \tilde{g}_4^* = 0$, with the eigenvalues $s_1 = -2$ and $s_2 = -1$ found at the tree level previously. Furthermore, there is a nontrivial fixed point at $\tilde{g}_2^* = -1/3$ and $\tilde{g}_4^* = 16\pi/3$. The matrix M now has the form

$$M = \begin{pmatrix} -2 & -\frac{1}{8\pi} \\ 0 & -1 + \frac{3\tilde{g}_4}{8\pi} \end{pmatrix}_{\tilde{g}_2^* = -1/3, \tilde{g}_4^* = 16\pi/3} = \begin{pmatrix} -2 & -\frac{1}{8\pi} \\ 0 & 1 \end{pmatrix} \quad (41)$$

Its eigenvalues are $s_1 = -2$ and $s_2 = 1$, so the fixed point is a saddle point or a hyperbolic point. It is called Wilson-Fisher (WF) fixed point. It appears in ϕ^4 models with dimension $2 < d < 4$. When $d \rightarrow 4$ then the WF fixed point tends to the origin and in $d = 4$ it melts into the GFP. Since the critical exponent ν of the correlation length ξ is identified as the negative reciprocal of the single negative eigenvalue of the matrix M coming from the linearization of the evolution equations, then it gives $\nu = -1/s_1 = 1/2$. The approximation of the model with two couplings makes the problem a mean field type one.

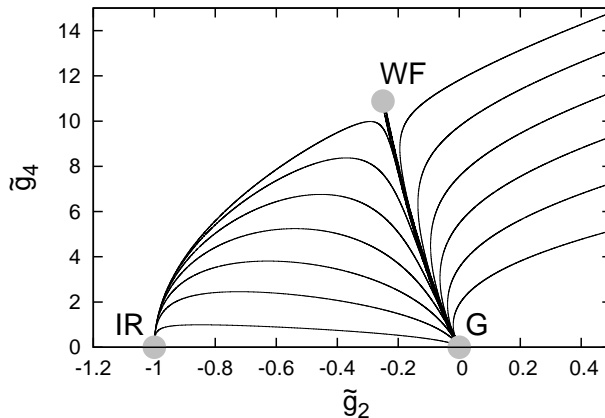


FIG. 4: The phase structure of the 3d ϕ^4 model calculated from the flow equations in Eq. (36). The model has a GFP, a WF and an IR fixed point. The latter one corresponds to a crossover fixed point between the UV and the IR ones.

The 3d ϕ^4 model has two phases. The trajectories tending right from the WF fixed point in Fig. 3 correspond to the symmetric phase. The trajectories tending left belong to the broken phase. There the Z_2 symmetry ($\phi \leftrightarrow -\phi$) is broken.

Further terms in the expansion in \tilde{g}_4 do not give further fixed points, but only changes qualitatively the position of the WF fixed point. If one considers the exact RG flow equations in the two couplings in Eq. (36) we have the GFP at the origin and the WF fixed point at $\tilde{g}_2^* = -1/4$ and $\tilde{g}_4^* = 2\sqrt{3}\pi$. The matrix M is

$$\begin{pmatrix} -2 + \frac{\tilde{g}_4}{16\pi(1+\tilde{g}_2)^{3/2}} & -\frac{1}{8\pi(1+\tilde{g}_2)^{1/2}} \\ -\frac{9\tilde{g}_4^2}{32\pi(1+\tilde{g}_2)^{5/2}} & -1 + \frac{3\tilde{g}_4}{8\pi(1+\tilde{g}_2)^{3/2}} \end{pmatrix}_{\tilde{g}_2^*=-1/4, \tilde{g}_4^*=2\sqrt{3}\pi} = \begin{pmatrix} -\frac{5}{3} & -\frac{1}{4\sqrt{3}\pi} \\ -4\sqrt{3}\pi & 1 \end{pmatrix}. \quad (42)$$

Its eigenvalues are $s_1 = -2$ and $s_2 = 4/3$. The WF fixed point remains a saddle point. The higher order terms in approximations (e.g. consideration of further couplings, inclusion wavefunction renormalization or even higher order terms in the derivative expansion) cannot change the type of the fixed point only the position is shifted further. We illustrate the phase structure in Fig. 4. Interestingly the trajectories tend to a single point in the broken phase. It might assume that there can be a further fixed point in the IR limit. That seems strange according to the β functions in Eq. (36), since we can find all the fixed point solutions analytically. The only possibility is that the ratios in Eq. (36) can tend to zero in the way that both the numerator and the denominator vanishes. If they are of the form of $0/0$, then it implies that the values of the couplings are $\tilde{g}_2^* = -1$ and $\tilde{g}_4^* = 0$. It corresponds to an effective potential of the form $\tilde{V}_0 = -\phi^2/2$. Clearly this fixed point cannot be reached by any expansions around the GFP since this point is a singular point of the evolution equations.

The effective potential of the symmetric phase can be handled quite easily numerically in contrast to the one in the broken phase, where one can face a very difficult numerical and theoretic problem [2]. The reason is that there is a condensate in the broken phase [81, 84, 121–124]. It can be considered as a macroscopic object constituting of a huge amount of soft modes. Its measure gives a dynamically appearing momentum scale in the model, which implies that there cannot be such modes which momentum is that is larger than the one characterizing the condensate [84, 114, 125]. The evolution stops when one reaches the scale of the condensate, which manifests in the form that the flows arrive at the singularity. Is there really a singularity there, or it is only a numerical artifact? It is known that the Wetterich equation in Eq. (12) should not drive the flows into singularity. However the approximation due to the strong truncation of the functional ansatz for the effective action, or in the derivative expansion may induce a singular behavior suggesting that the singularity is a numerical artifact. Therefore it is argued that the singularity can be avoided by a proper choice of the IR regulator, and the flow can reach arbitrarily small scales. However it was shown for a huge set of scalar models [29, 48, 86, 87] that such a singularity possesses a specific scaling behavior induced by the IR fixed point, therefore it may have a significant physical importance. The singularity in the RG evolution is always reached, but the RG equations do not loose their validity, they simply stop at a finite scale [44, 126]. This finite scale also appears when it seems that the evolution avoids the singularity with special regulators. In those cases, after an abrupt change in the scaling of the couplings, a marginal scaling appears towards the deep IR regime without any universality. Therefore the dynamically appearing finite momentum scale seems to be the only universal behavior in the IR.

The dynamical scale is induced by an IR fixed point in the broken phase. One can determine numerically the critical exponents in its vicinity. The IR fixed point can be uncovered analytically from the β function in Eq. (36) by reparametrization of the couplings according to $\omega = 1 + \tilde{g}_2$, $\chi = \tilde{g}_4/\omega$ and $\partial_\tau = \omega \partial_t$. We obtain that

$$\begin{aligned}\partial_\tau \omega &= 2\omega(1 - \omega) - \frac{\chi\omega}{8\pi}, \\ \partial_\tau \chi &= -\chi + \frac{\chi^2}{4\pi}.\end{aligned}\tag{43}$$

The reparametrized flow equations give the Gaussian ($\omega_G^* = 1$, $\chi_G^* = 0$), and the WF ($\omega_{WF}^* = 3/4$, $\chi_{WF}^* = 4\pi$) fixed points, however another one appears at $\omega_{IR}^* = 0$ and $\chi_{IR}^* = 4\pi$. The latter can be identified with the IR fixed point where the trajectories of the broken phase meet. The corresponding eigenvalues are $s_1 = 1$ and $s_2 = 3/2$ expressing the UV repulsive (IR attractive) nature of the IR fixed point.

The determination of the critical exponents in the vicinity of the IR fixed point is demonstrated in the framework of the d -dimensional $O(N)$ model. The potential has the form

$$\tilde{V} = \sum_{n=2}^{N_\lambda} \frac{\lambda_n}{n!} (\rho - \kappa)^n,\tag{44}$$

with N_λ the degree of the Taylor expansion and the dimensionless couplings κ and λ_n for $n \geq 2$. For shorthand we use $\lambda_2 = \lambda$. The further dimensionless quantities are denoted by \sim . The introduction of the coupling κ serves a better convergence in the broken symmetric phase. The evolution equation for the potential reads as

$$k\partial_k \tilde{V} = -d\tilde{V} + (d-2+\eta)\tilde{\rho}\tilde{V}' + \frac{4vd}{d} \left(1 - \frac{\eta}{d+2}\right) \left(\frac{1}{1+\tilde{V}'+2\tilde{\rho}\tilde{V}''} + \frac{N-1}{1+\tilde{V}'}\right),\tag{45}$$

by using Litim's regulator, with the notation $' = \delta/\delta\rho$. In Eq. (45) we introduced the anomalous dimension η which is defined via the wavefunction renormalization according to $\eta = -d\log Z/d\log k$ and can be calculated by means of the couplings as

$$\eta = \frac{16vd}{d} \frac{\kappa\lambda^2}{1+2\kappa\lambda}.\tag{46}$$

The inclusion of η in the RG equation mimics the evolution of the wavefunction renormalization. We note that a more precise treatment can be obtained if one Taylor expand the evolution equation for Z in Eq. (17). Again, we start with the 3d $O(1)$ model. It is instructive to retreat the phase structure, since the IR fixed point moves to infinity. Now its flow equations are

$$\begin{aligned}\dot{\kappa} &= -\kappa + \frac{1}{2\pi^2(1+2\kappa\lambda)^2}, \\ \dot{\lambda} &= -\lambda + \frac{3\lambda^2}{\pi^2(1+2\kappa\lambda)^3},\end{aligned}\tag{47}$$

for the first two couplings if we set $\eta = 0$ and $\lambda_n = 0$ for $n > 2$. The $O(N)$ model in $d = 3$ has two phases. The typical phase structure is depicted in Fig. 5 for the couplings in Eq. (47). From the flow equations in Eq. (47) one can find two fixed points in the model. The Gaussian fixed point can be found at $\kappa_G^* = 1/2\pi^2$ and $\lambda_G^* = 0$, although it is not situated in the origin due to the redefinition of the field variable. The linearization of the flow equations around the GFP gives a matrix with negative eigenvalues ($s_{G1} = -1$ and $s_{G2} = -1$), i.e. the fixed point is repulsive or UV attractive. The WF fixed point can be found at the values of the couplings $\kappa_{WF}^* = 2/9\pi^2$ and $\lambda_{WF}^* = 9\pi^2/8$, with eigenvalues $s_{WF1} = 1/3$ and $s_{WF2} = -2$, so it is a hyperbolic point.

We usually identify the critical exponent ν of the correlation length ξ in the vicinity of the WF fixed point by taking the negative reciprocal of the single negative eigenvalue, which gives $\eta_{WF} = 1/2$ in this case. Let us notice that the flows tend to a single curve beyond the WF fixed point in the broken phase into the IR fixed point at $\kappa_{IR}^* \rightarrow -\infty$ and $\lambda_{IR}^* = 0$. Again, with the help of a rescaling of the couplings the attractive IR fixed point can be uncovered and one finds the following pair of evolution equations

$$\begin{aligned}\partial_\tau \omega &= 2\omega(1 - \omega) - \frac{\ell\omega}{\pi^2}(3 - 4\omega), \\ \partial_\tau \ell &= \ell(5\omega - 6) + \frac{9\ell^2}{\pi^2}(1 - \omega),\end{aligned}\tag{48}$$

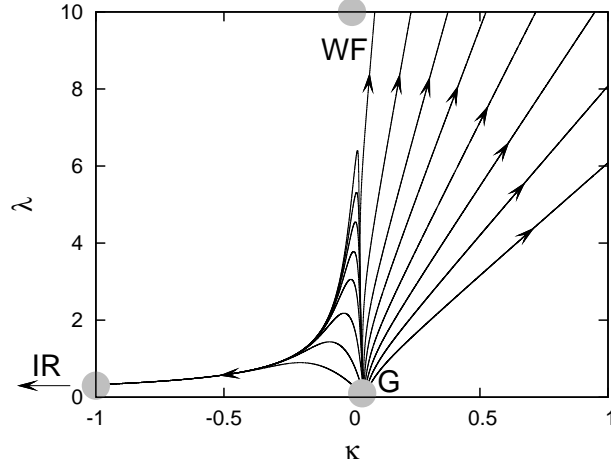


FIG. 5: The phase space of the 3d $O(N)$ model is shown. The flows belonging to the symmetric (broken symmetric) phase tend to right (left), respectively. Again, the Wilson-Fisher fixed point plays the role of the crossover fixed point between the UV (which is now the Gaussian) and the IR ones.

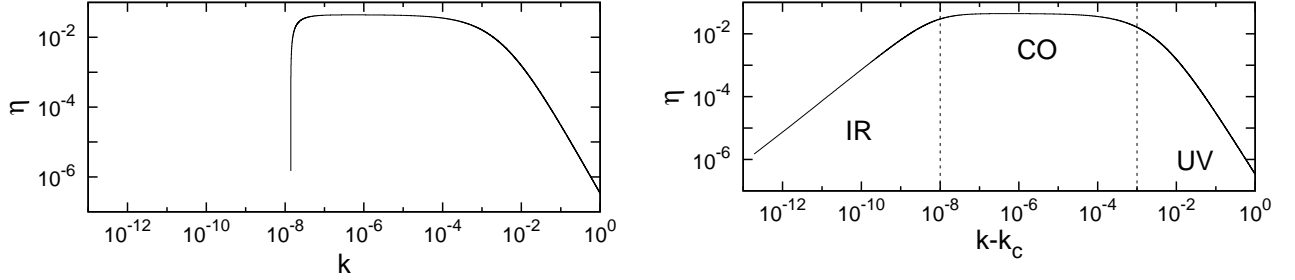


FIG. 6: The evolution of the anomalous dimension η is presented. In the left figure the flow of η shows a strong singularity as the function of the scale k , while this singularity becomes a power law like convergence as the function of the shifted scale $k - k_c$ in the right one.

where $\omega = 1 + 2\kappa\lambda$, $\ell = \lambda/\omega^3$ and $\partial_\tau = k\partial_k/\omega$. The static equations now have the Gaussian ($\ell_G^* = 0$, $\omega_G^* = 1$), the WF ($\ell_{WF}^* = \pi^2/3$, $\omega_{WF}^* = 3/2$) and the IR ($\ell_{IR}^* = 2\pi^2/3$, $\omega_{IR}^* = 0$) fixed point solutions. Naturally the Gaussian and the WF ones has the same behavior as was obtained from direct calculations. However the new IR fixed point indeed corresponds to the values $\kappa_{IR}^* \rightarrow -\infty$ and $\lambda_{IR}^* = 0$, and the linearization in its vicinity gives the eigenvalues $s'_{IR1} = 6$ and $s'_{IR2} = 0$, a positive and a zero one, showing that the fixed point is IR attractive, in accordance with the flows in Fig. 5.

If we let many couplings and η evolve, then the phase space does not change significantly, but the IR fixed point can be observed more easily. In order to demonstrate it we plotted the flow of the anomalous dimension in Fig. 6. We also plotted η as the function of the shifted scale $k - k_c$ in the right figure of Fig. 6. In the UV region the Gaussian fixed point drives the evolution of the anomalous dimension. In this regime it grows according to the power law scaling $\eta_{UV} \sim (k - k_c)^{-2}$. There is a crossover (CO) scaling region between $10^{-8} \lesssim k - k_c \lesssim 10^{-4}$ where a plateau appears giving a constant value for $\eta_{CO} \approx 0.043$ due to the WF fixed point. Going further in the evolution towards the smaller values of k below $k - k_c \sim 10^{-8}$ one can find a third scaling regime. It appears a simple singularity in the left figure, but the shifted scale $k - k_c$ clearly uncovers the power law scaling of the anomalous dimension there according to $\eta_{IR} \sim (k - k_c)^1$. This scaling region is induced by the IR fixed point.

The evolution of the other couplings also shows such type of scaling regimes with similar singularity structure in the IR limit. There the power law scaling behaviors also take place as the function of $k - k_c$ with the corresponding exponents. This suggests that the appearing singularities are not artifacts and the RG flows can be traced till the value of k_c .

We note that one can find such a value of N_λ where the evolution does not stop as in the upper figure in Fig. 6, but after a sharp fall during the flow of η it continues its RG evolution marginally giving a tiny value there. However, the singular-like fall possesses the same power-law like behavior as the function of $k - k_c$, for any value of N_λ . It suggests

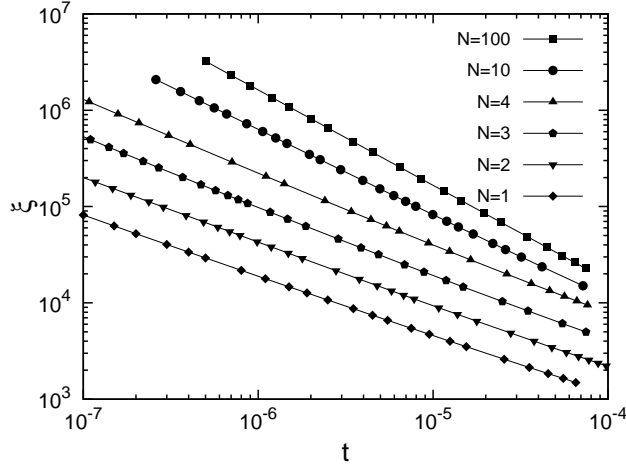


FIG. 7: The scaling of the correlation length ξ as the function of the reduced temperature t , for various values of N .

N	1	2	3	4	10	100
ν_{IR}	0.624	0.666	0.715	0.760	0.883	0.990
ν_{WF}	0.631	0.666	0.704	0.739	0.881	0.990

TABLE I: The critical exponent ν in the $O(N)$ model for various values of N .

that the value of η rapidly falls to zero at k_c and it is due to the numerical inaccuracy, whether the RG evolution survives the falling and can be traced to any value of k , or the flows stop due to the appearing singularity. It strongly suggests that the singular behavior with its uncovered IR scaling for the shifted scale $k - k_c$ is not an artifact but is of physical importance, since the value of the scale k_c , which appears there can characterize the condensate as the smallest available scale. If one tunes the initial values of the couplings κ_{k_Λ} , λ_{k_Λ} etc., to the separatrix then the value of k_c decreases. It enables us to define the correlation length ξ in the IR scaling regime as the reciprocal of the scale where the evolution stops, i.e. $\xi = 1/k_c$. As the initial couplings approach the separatrix the stopping scale $k_c \rightarrow 0$ therefore the correlation length diverges. Naturally it is infinite in the symmetric phase. We can identify the reduced temperature t in the $O(N)$ model as the deviation of the UV coupling κ_{k_Λ} to its UV critical value, i.e. $t \sim \kappa_{k_\Lambda}^c - \kappa_{k_\Lambda}$. By starting evolutions for different values of the UV coupling κ_{k_Λ} then one can get the corresponding values ξ . One should fine tune the initial coupling to get larger and larger values of ξ to reach the IR scaling regime. The critical initial value of $\kappa_{k_\Lambda}^c$ can be determined by the trick, where one should fine tune its value in the log-log plot of the t, ξ plane till one obtains a straight line there. This holds for continuous phase transition. The absolute value of the negative slope of the line provides us the exponent ν corresponding to the correlation length.

In the 3d $O(N)$ model a second order or continuous phase transition appears according to the power law scaling

$$\xi \sim t^{-\nu}. \quad (49)$$

The results are plotted in Fig. 7. For a given value of N we obtain power-law like behavior for the scaling of ξ , and the slope of the line provides the exponent ν in the log-log scale. The obtained results are listed in Table I. We denoted the WF (IR) values of ν as ν_{WF} (ν_{IR}), respectively. The results show high coincidence. The values ν_{WF} are taken from results obtained from derivative expansion up to the second order, since this approximation is the closest to our treatment. One can conclude that the exponent ν can be also determined from the scaling around the IR fixed point, and has the same value as was obtained around the WF fixed point.

In arbitrary dimensions one can consider the evolution of the couplings κ and λ around the GFP. It is situated at $\kappa_G^* = 2^{1-d}\pi^{-d/2}(N+2)/d(d-2)\Gamma(d/2)$ and $\lambda_G^* = 0$. The corresponding matrix M is

$$M = \begin{pmatrix} 2-d & \frac{3(N+2)4^{1-d}\pi^{-d}}{d-2\Gamma(1+d/2)^2} \\ 0 & d-4 \end{pmatrix}, \quad (50)$$

therefore the eigenvalues are $s_{G1} = 2-d$ and $s_{G2} = d-4$. When $2 < d < 4$, then the GFP is UV attractive and the model is asymptotically free. However one of the eigenvalues become zero at $d=4$, and the coupling λ does not

necessarily converge to zero, and the model is not asymptotically free anymore. The appearing divergence can be related to the Landau pole, where a singularity of the couplings appears at a finite scale k , as e.g. in QED [58, 127].

III. ASYMPTOTIC SAFETY

The concept of perturbative renormalizability and the asymptotic freedom is restricted to the GFP. It guarantees that the physical quantities which are calculated from the model do not suffer from divergences. However if there are irrelevant couplings in the GFP which are crucial in describing the model that is investigated, (e.g. the Newton constant in QEG, which makes the GFP a hyperbolic one) then the systematic removal of the divergences may even induce infinitely many new important couplings which implies that the model disables us to give any physical predictions.

However there can be further nontrivial (non-Gaussian) fixed points (NGFP), where the physically important couplings are relevant, which means that the theory can give finite physical quantities. This is the basic idea of the asymptotic safety. In general sense the asymptotic safety means that the theory is free from divergences if the cutoff is removed to infinity assuming that the corresponding fixed point possesses a finite number of UV attractive directions. In the fixed point those couplings should scale in relevant manner which are crucial to obtain finite physical quantities. Naturally there can be certain couplings which are generated by the RG procedure, but has no physical meaning. It is necessary to have finite number of relevant couplings, otherwise every trajectory would tend to the fixed point and the theory would not be predictive. The definition of the asymptotic safety is not restricted to the GFP. It implies that there is a UV NGFP in the phase space. The asymptotic safety requires that the eigenvalues corresponding to the linearized RG flows of the physically important couplings around the UV NGFP should have negative real parts.

Examples for asymptotically safe theories are e.g. quantum gravity, the Gross-Neveu and the nonlinear σ models with dimension $2 < d < 4$, or the 2d sine-Gordon model.

A. The nonlinear σ model

The nonlinear σ model (NLSM) in general describes the dynamics of a map φ from a d -dimensional manifold \mathcal{M} to a N -dimensional manifold \mathcal{N} . The model is renormalizable in $d = 2$ and is asymptotically free [128, 129]. However if one goes beyond $d = 2$ then it becomes nonrenormalizable since the existing UV attractive Gaussian fixed point becomes a hyperbolic one. However a nontrivial UV fixed point arises [128], which saves the UV limit, and the model becomes asymptotically safe. The action of the model contains only derivative interactions, e.g.

$$S = \frac{1}{2}\zeta \int d^d x \partial_\mu \varphi^\alpha \partial^\mu \varphi^\beta h_{\alpha\beta}(\varphi) \quad (51)$$

where $h_{\alpha\beta}$ is the dimensionless metric, $\zeta = 1/g_0^2$ and its dimension is $[g_0] = k^{(2-d)/2}$. The RG equations can be derived by background field method. The perturbative RG flow gives [72]

$$\beta_{\tilde{g}_0} = \frac{d-2}{2}\tilde{g}_0 - c_d \frac{R}{N} \tilde{g}_0^3, \quad (52)$$

with

$$c_d = \frac{1}{(4\pi)^{d/2} \Gamma(d/2 + 1)}. \quad (53)$$

There are two fixed point of the flow equation in Eq. (52). At $g_{0G}^* = 0$ we have a GFP, with the eigenvalue $s_G = (d-2)/2$. It is clearly positive for $d > 2$ giving irrelevant scalings and divergences in the UV limit. The other fixed point is situated at $g_{0UV}^{*2} = (d-2)N/(2c_d N)$ giving the eigenvalue $s_{UV} = 2-d$, which induces relevant scaling, therefore the NLSM exhibits asymptotic safety, yet at perturbative level. The critical exponent ν of the correlation length ξ equals the negative reciprocal of s_{UV} giving $\nu = 1/(d-2)$.

The functional RG flow equation results in the equation [72]

$$\beta_{\tilde{g}_0} = \frac{d-2}{2}\tilde{g}_0 - \frac{c_d \frac{R}{N} \tilde{g}_0^3}{1 - 2c_d \frac{R}{N(d+2)} \tilde{g}_0^2}. \quad (54)$$

Again, we have two fixed points. The origin is a GFP with the same eigenvalue $s_G = (d-2)/2$, and we have a UV NGFP at $g_{0UV}^{*2} = N(d^2 - 4)/(4c_d d R)$. It is an UV attractive point with eigenvalue $s_{UV} = -2d(d-2)/(d+2)$. We

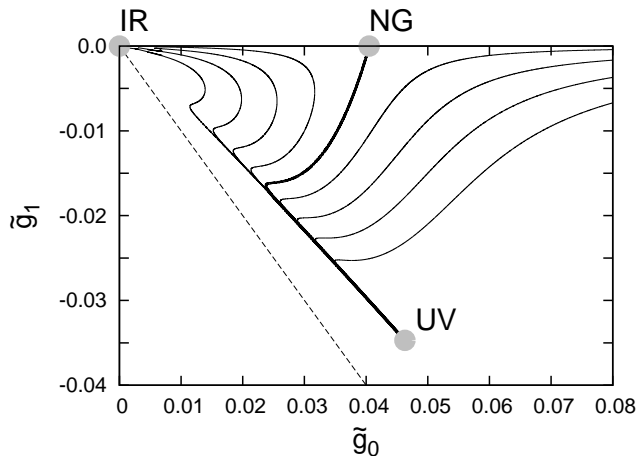


FIG. 8: The phase space of the nonlinear σ model is presented. The trajectories tending to the left towards the IR fixed point are in the broken phase, the others belong to the symmetric phase. The fixed points are denoted by gray points, they are: UV attractive NGFP \rightarrow UV, hyperbolic NGFP \rightarrow NG, and IR fixed point \rightarrow IR. The separatrix is situated between the UV and the NG fixed points, and is denoted by the thick line. The latter is a saddle point and plays the role of the crossover fixed point in this model. The dashed line shows the singularity limit, when $\tilde{g}_0 = -\tilde{g}_1$.

note that this value is smaller than the one that was obtained perturbatively, therefore the exponent ν is greater, e.g. it is $\nu = 5/6$, when $d = 3$. In the NLSM the perturbative and the exact RG flow equations give qualitatively similar results, and the functional RG method changes only the position of the fixed points, and the concrete value of exponents. The asymptotic safety appears in both the perturbative and the exact RG treatments.

Taking into account more interacting terms in the action in Eq. (51) we should introduce further couplings in the model [130]. The β functions for two couplings reads as

$$\begin{aligned}\tilde{\beta}_{\tilde{g}_0} &= \tilde{g}_0 + \tilde{g}_0(N-2)\tilde{Q}_{d/2,2} + d\tilde{g}_1(N-2)\tilde{Q}_{d/2+1,2}, \\ \tilde{\beta}_{\tilde{g}_1} &= -\tilde{g}_1 + \tilde{g}_1(N-2)\tilde{Q}_{d/2,2},\end{aligned}\quad (55)$$

where

$$\tilde{Q}_{n,l} = \frac{1}{(4\pi)^{d/2}\Gamma(n)} \left(\frac{(2n+2+\partial_t)\tilde{g}_0}{n(n+1)(\tilde{g}_0+\tilde{g}_1)^l} + \frac{2(2n+4+\partial_t)\tilde{g}_1}{n(n+2)(\tilde{g}_0+\tilde{g}_1)^l} \right). \quad (56)$$

The phase structure is given in Fig. 8. The model has two phases henceforward, but new fixed points appear. At $\tilde{g}_{0NG} = 2/5\pi^2$ and $\tilde{g}_{1NG} = 0$ a hyperbolic NGFP appears. The trajectories are UV attracted from the direction of \tilde{g}_0 and UV repelled from \tilde{g}_1 . It implies that including a new coupling into the model the asymptotic safety obtained for a single coupling disappears. The eigenvalues are $s_{NG0} = -6/5$ and $s_{NG1} = 2$. The former gives $\nu = -1/s_{NG0} = 5/6$ for the critical exponent, which coincides with the one obtained for \tilde{g}_0 alone. However a further NGFP appears at $\tilde{g}_{UV0}^* = 16/35\pi^2$ and $\tilde{g}_{UV1}^* = -12/35\pi^2$. The new fixed point is UV attractive as the flows show in Fig. 8, the eigenvalues are $s_{UV0} = -0.457$ and $s_{UV1} = -13.11$. Let us mention, that a further hyperbolic fixed point appears in the phase space far from the region shown in Fig. 8. Noticeably the trajectories meet at the GFP in the broken phase, if one follows the evolutions into the deep IR region, see Fig. 8.

According to the β functions in Eq. (55) the quantity $\tilde{g}_0 + \tilde{g}_1 = 0$ makes the flows singular. We plotted it for different UV initial values of the couplings in Fig. 9. The trajectories have three different scaling regimes. In the UV there is a short, relevant scaling region induced by the UV attractive NGFP. Then the scalings become marginal in the vicinity of the hyperbolic NGFP. In the IR region the trajectories belonging to the symmetric phase diverge as k^1 . In the broken phase the flows tend to zero sharply at a certain scale k_c , which can be identified with the correlation length ξ again. Therefore one can determine the exponent ν of ξ in the IR. It gives $\nu = 0.835$, which is very close to the value $\nu = 5/6$, that was got analytically in the vicinity of the hyperbolic NGFP.

B. The Gross-Neveu model

The Gross-Neveu (GN) model is a 2-dimensional quantum field theoretic model of N_f flavors of massless relativistic fermions which interact via a four-fermionic term [131]. The model is asymptotically free. The GN model was also

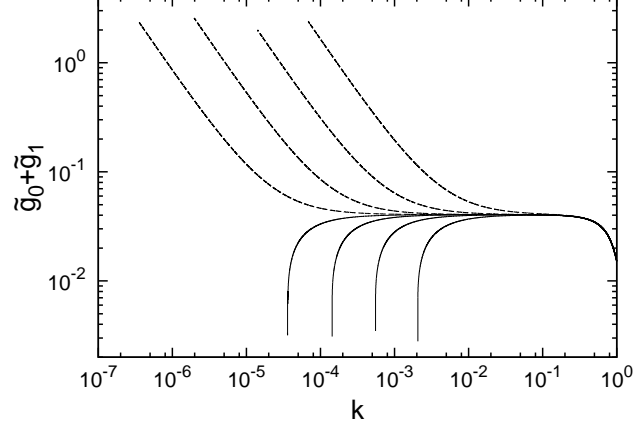


FIG. 9: The flow of the quantity $\tilde{g}_0 + \tilde{g}_1$ is shown. The full (dashed) line corresponds to evolutions in the broken (symmetric) phase, respectively.

investigated at finite chemical potential in $d = 2$, where an analytic solution of the crystal ground state is found [132]. In $d = 3$ the model is not asymptotically free [85]. It can also be studied at finite temperature [52] and chemical potential [133]. The Euclidean effective action of the GN model has the form [85]

$$S[\bar{\psi}, \psi] = \int_x \left[Z_\psi \bar{\psi} i \not{\partial} \psi + \frac{\bar{g}}{2N_f} (\bar{\psi} \psi)^2 \right], \quad (57)$$

with the wavefunction renormalization Z_ψ which is set to $Z_\psi = 1$ in LPA. The dimensionless four-fermion coupling g can be obtained from the dimensionful \bar{g} as

$$g = Z_\psi^{-2} k^{d-2} \bar{g}. \quad (58)$$

The functional RG treatment of the GN model leads to the RG flow equation

$$\beta_g = (d - 2 + 2\eta_\psi)g - 4d_\gamma v_d l_1^F(0)g^2 \quad (59)$$

in the $N_f \rightarrow \infty$ limit [85]. The constant d_γ denotes the dimension of the Dirac-algebra, e.g. it is $d_\gamma = 4$ when $d = 3$. The other constant $l_1^F(0)$ is an IR regulator dependent quantity, for example $l_1^F(0) = 2/d$ when one uses the Litim's regulator. The model has two fixed points. We have a GFP at $g^* = 0$ with the eigenvalue $s_G = d - 2$. It shows that the four-fermion coupling multiplies an irrelevant operator, thus the model is perturbatively nonrenormalizable. The other NGFP is situated at

$$g^* = \frac{d - 2 + 2\eta_\psi}{4d_\gamma v_d l_1^F(0)}, \quad (60)$$

which, by using Litim's regulator in LPA and considering $d = 3$ becomes $g^* = 3\pi^2/4$. Its corresponding eigenvalue is $s_{UV} = 2 - d$, which gives a relevant coupling when $d > 2$, so this fixed point is a UV attractive NGFP. In the case of $d = 2$ the model is asymptotically free, perturbatively renormalizable with its UV attractive GFP.

In the partially bosonized version of the GN model [52, 85, 134] a hyperbolic fixed point, and a UV attractive GFP appears, so the model becomes asymptotically free. From [85] the corresponding evolution equations for the d -dimensional bosonized GN model is

$$\dot{u} = -du + (d - 2 + \eta_\sigma)u'\rho - 2d_\gamma v_d l_0^{(F)d}(2h^2\rho; \eta_\psi) + \frac{1}{N_f} 2v_d l_0^d(u' + 2\rho u''; \eta_\sigma), \quad (61)$$

where we impose a polynomial ansatz for the potential

$$u(\rho) = \sum_{n=0}^{\infty} \frac{\lambda_{2n}}{n!} \rho^n, \quad (62)$$

with the bosonic couplings λ_{2n} . One can relate the coupling g in Eq. (59) as $g = h^2/\lambda_2$. The flow equation for the Yukawa coupling is

$$\dot{h}^2 = (d - 4 + 2\eta_\psi + \eta_\sigma)h^2 + \frac{1}{N_f}8v_d h^4 l_{1,1}^{(FB)d}(0, \lambda_2; \eta_\psi, \eta_\sigma). \quad (63)$$

The anomalous dimensions are

$$\begin{aligned} \eta_\sigma &= 8\frac{d_\gamma v_d}{d}h^2 m_4^{(F)d}(0; \eta_\psi), \\ \eta_\psi &= \frac{1}{N_f}8\frac{v_d}{d}h^2 m_{1,2}^{(FB)d}(0, \lambda_2; \eta_\psi, \eta_\sigma). \end{aligned} \quad (64)$$

We introduced the threshold functions

$$\begin{aligned} l_0^d(\omega; \eta_\sigma) &= \frac{2}{d} \left(1 - \frac{\eta_\sigma}{d+2}\right) \frac{1}{1+\omega}, \\ l_0^{(F)d}(\omega; \eta_\psi) &= \frac{2}{d} \left(1 - \frac{\eta_\psi}{d+2}\right) \frac{1}{1+\omega}, \\ l_{1,1}^{(FB)d}(\omega_1, \omega_2; \eta_\psi, \eta_\sigma) &= \frac{2}{d} \frac{1}{(1+\omega_1)(1+\omega_2)} \left\{ \left(1 - \frac{\eta_\psi}{d+1}\right) \frac{1}{1+\omega_1} + \left(1 - \frac{\eta_\sigma}{d+2}\right) \frac{1}{1+\omega_2} \right\}, \\ m_4^{(F)d}(\omega; \eta_\psi) &= \frac{1}{(1+\omega)^4} + \frac{1-\eta_\psi}{d-2} \frac{1}{(1+\omega)^3} - \left(\frac{1-\eta_\psi}{2d-4} + \frac{1}{4}\right) \frac{1}{(1+\omega)^2}, \\ m_{1,2}^{(FB)d}(\omega_1, \omega_2; \eta_\psi, \eta_\sigma) &= \left(1 - \frac{\eta_\sigma}{d+1}\right) \frac{1}{(1+\omega_1)(1+\omega_2)^2}. \end{aligned} \quad (65)$$

Keeping only the couplings h^2 and λ_2 we get the evolution equations for $d = 3$

$$\begin{aligned} \dot{\lambda}_2 &= -2\lambda_2 + \frac{4}{3\pi^2}h^2 + \frac{5}{3\pi^2}h^2\lambda_2, \\ \dot{h}^2 &= -h^2 + \frac{5}{3\pi^2}h^4 + \frac{2h^4(2+\lambda_2) - \frac{2}{9\pi^2}h^6}{N_f 3\pi^2(1+\lambda_2)^2}. \end{aligned} \quad (66)$$

The flow equations have a UV attractive GFP at the origin at $h_G^{2*} = 0$ and $\lambda_{2G}^* = 0$ and a non-Gaussian saddle point at $h_{NG}^{2*} = 5.764$ and $\lambda_{2NG}^* = 0.758$ for $N_f = 12$. The phase structure can be seen in Fig. 10. The trajectories tending to left and right correspond to regions of different phases in the model. After the reparametrization of the couplings

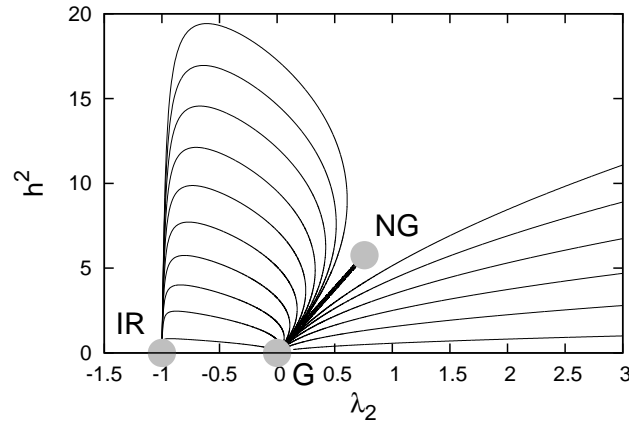


FIG. 10: The phase space of the 3d Gross-Neveu model is shown. The trajectories tending to the IR fixed point are in the broken phase, the others belong to the symmetric phase. The fixed points are denoted by gray points. The separatrix between the phases is represented by the thick line and connects the Gaussian (G) and the non-Gaussian (NG) fixed points. The GFP is a UV attractive, the hyperbolic NGFP is a crossover fixed point.

N	1	2	6	12	50
ν_{IR}	0.922	0.976	0.990	0.996	1.00

TABLE II: The critical exponent ν in the 3d Gross-Neveu model for various values of N .

according to $\omega = 1 + \lambda_2$, $\chi = h^2/\omega$ and $\partial_\tau = \omega\partial_t$ we get

$$\begin{aligned}\partial_\tau\omega &= 2\omega(1-\omega) + \frac{\chi\omega^2}{3\pi^2}(5\omega-1), \\ \partial_\tau\chi &= 2\chi(\omega-2) + \frac{\chi^2}{18\pi^2}\left(7\omega+1-\frac{\chi\omega}{3\pi^2}\right).\end{aligned}\quad (67)$$

The new flow equations have three physical fixed points. The UV attractive GFP can be found at $\omega_G^* = 1$ and $\chi_G^* = 0$. The NGFP is situated at $\omega_{NG}^* = 1.758$ and $\chi_{NG}^* = 3.278$ with a positive and a negative eigenvalues. There is a third fixed point at $\omega_{IR}^* = 0$ and $\chi_{IR}^* = 355.206$ with two positive eigenvalues implying that that this fixed point is a UV repulsive or IR attractive, therefore we can identify it with the IR fixed point at $h_{IR}^{2*} = 0$ and $\lambda_{2IR}^* = -1$ if we express them in terms of the original couplings. One can investigate the scaling of the couplings in the vicinity of the IR fixed point, and it is shown in Fig. 11.

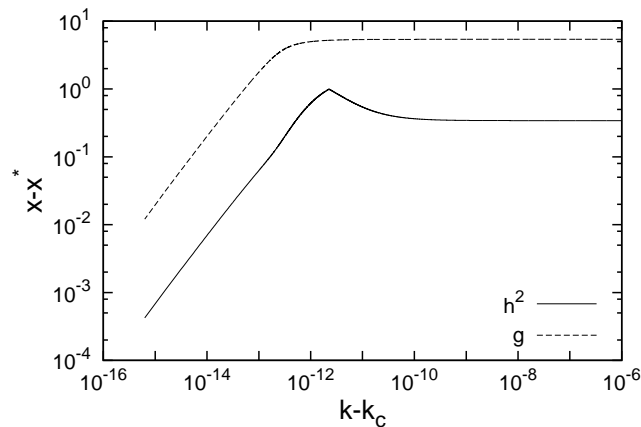


FIG. 11: The scaling of the couplings in the 3d Gross-Neveu model is shown, x denotes h_2 and λ_2 , the fixed points values are $h_2^* = 0$ and $\lambda_2^* = -1$. The couplings have a long marginal scaling region induced by the hyperbolic NGFP. In the IR limit there is another scaling regime, which can be uncovered by using the shifted scale $k - k_c$.

The couplings are constants in the beginning of the flows, giving marginal scaling due to the hyperbolic NGFP in Fig. 10, that is $x - x^* \sim (k - k_c)^0$. In the deep IR region the couplings have singular behaviors, i.e. they abruptly become zero or infinite at a certain scale k_c . If one plots the couplings as the function of the shifted scale $k - k_c$, then one can obtain a power-law like behavior according to $x - x^* \sim (k - k_c)^1$, where x^* is the fixed point value of the couplings, for example $h_2^* = 0$ and $\lambda_2^* = -1$, see Fig. 11. It implies that the original four-fermion coupling g tends to zero in the IR limit. We also calculated the critical exponent ν of the correlation length in the IR regime by the previously shown method, which is based on identifying the correlation length by the reciprocal of the stopping scale k_c . The results are summarized in Table II. They show good coincidence with the ones obtained in [53].

C. The 2d sine-Gordon model

The 2d sine-Gordon model can be an example for asymptotic freedom and asymptotic safety, simultaneously. Its effective action contains a sinusoidal potential of the form

$$\Gamma_k = \int \left[\frac{z}{2} (\partial_\mu \phi)^2 + u \cos \phi \right], \quad (68)$$

where z is the field independent wavefunction renormalization and u is the coupling. The perturbative RG results beyond LPA [26] can account for the KT phase transition and give $1/z \rightarrow 0$ for $1/z < 8\pi$ in the IR limit. By using the flow equation approach [135, 136] a different IR limit is obtained for the frequency, i.e. $1/z \rightarrow 4\pi$. However we note, that this method cannot recover the leading order perturbative UV results for $1/z < 4\pi$, due to the opposite sign obtained for the evolution equation for the frequency. Functional RG approaches can map the phase structure of the SG model in LPA [80, 81, 126, 137–139] and can also take into account the evolution of the wavefunction renormalization [28, 29, 140–142].

Besides the Z_2 symmetry the model has a periodic symmetry. The model has two phases. The effective potential should be convex (nonconcave), furthermore the RG equations should not break the periodic symmetry, too. This two requirements can be satisfied if the effective potential is flat, or zero [80, 143]. Then how one can distinguish the phases in the model? The simple answer is that one should consider the dimensionless effective potential, since only the dimensionful one should be convex. In the symmetric phase the dimensionless effective potential is flat, while it is a concave function in the broken phase. In LPA we got that it is $\tilde{V}_0 = -\phi^2/2$, which is repeated periodically in the field variable. This result can be obtained if one considers the evolution of higher harmonics in the potential, or if one follows the flow of the potential without its Fourier expansion.

The phases cannot be always distinguished by the form of the effective potential. The real difference comes from the property how the effective potential depends on the UV initial value of the couplings. It seems to contradict to the fact that the effective potential is a simple function at $k = 0$. However this scale cannot be reached, since during the evolution we use that the ratio $\Delta k/k$ is small disabling us to reach the exact value of $k = 0$. If we consider the RG time t then it is more apparent that we have only tendencies to infinity. Therefore it is meaningful to investigate how the asymptotic behavior of the effective action becomes the effective potential when the scale k is lowered. One can observe that a power law scaling appears in the deep region IR which can imply that the appearing scaling behavior can be extrapolated to $k = 0$. In the case of the 2d SG model the effective potential in the symmetric phase depends on the initial value of $\tilde{u}(k_\Lambda)$, while it is universal (independent on the initial coupling) in the broken phase. This type of separation of phases always works in any models.

1. Local potential approximation

By using the power law IR regulator in Eq. (6) with the choice $b = 1$ the leading order approximation of the RG evolution equations is

$$\begin{aligned}\dot{\tilde{u}} &= -2\tilde{u}, \\ \dot{z} &= 0.\end{aligned}\tag{69}$$

These equations are usually referred to as UV scalings. The fixed points are $\tilde{u}^* = 0$ with arbitrary z^* . These points constitute a line of fixed points. Since z does not evolve, then we are in LPA. The matrix M corresponding to the linearized RG equations in the vicinity of the line of fixed points is

$$\begin{pmatrix} -2 + \frac{1}{4\pi z} & -\frac{\tilde{u}}{4\pi z^2} \\ 0 & 0 \end{pmatrix}_{\tilde{u}^*=0, z^*} = \begin{pmatrix} -2 + \frac{1}{4\pi z^*} & 0 \\ 0 & 0 \end{pmatrix}\tag{70}$$

The eigenvalue to the evolution of \tilde{u} is $s = -2 + \frac{1}{4\pi z^*}$. Its sign depends on the value of z^* . If $z^* < 1/8\pi$ then $s > 0$ and the coupling is irrelevant. When $z^* > 1/8\pi$ then $s < 0$ and the coupling scales in relevant manner. These two types of scalings gives the two phases of the model separated by the critical value $z_c^* = 1/8\pi$. The point $\tilde{u}_c^* = 0$ and $z_c^* = 1/8\pi$ is called the Coleman point. The separatrix is a vertical line and goes through the Coleman point in the phase space.

The symmetric phase, when $z^* < 1/8\pi$ the phase is usually called the nonrenormalizable (or massless) phase due to the irrelevant scaling of the coupling \tilde{u} . The other phase is the broken one. There the Z_2 symmetry breaks down, it is called the renormalizable (or massive) phase (\tilde{u} is relevant there).

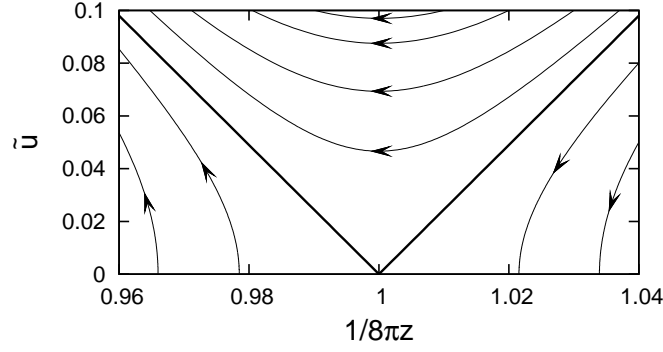


FIG. 12: The phase structure of the 2d sine-Gordon model treated in linear approximation. The separatrix is denoted by a thick line.

2. Linearized RG equations

By using the power law IR regulator in Eq. (6) with the choice $b = 1$ the linearized RG evolution equations are

$$\begin{aligned}\dot{\tilde{u}} &= \tilde{u} \left(-2 + \frac{1}{4\pi z} \right) + \mathcal{O}(\tilde{u}^2), \\ \dot{z} &= -\frac{\tilde{u}^2}{24\pi} + \mathcal{O}(\tilde{u}^3).\end{aligned}\quad (71)$$

The fixed point solution is $\tilde{u}^* = 0$ and z^* arbitrary. The matrix M is

$$\left(\begin{array}{cc} -2 + \frac{1}{4\pi z} & -\frac{\tilde{u}}{4\pi z^2} \\ -\frac{\tilde{u}}{12\pi} & 0 \end{array} \right)_{\tilde{u}^*=0, z^*} = \left(\begin{array}{cc} -2 + \frac{1}{4\pi z^*} & 0 \\ 0 & 0 \end{array} \right).\quad (72)$$

In case of the linear approximation the wavefunction renormalization z does not evolve, similarly to the LPA case, and we also have the same eigenvalues. It also implies that in the vicinity of the line of fixed points z does not evolve, which is reflected by perpendicular trajectories to the horizontal axis. The eigenvalues are the same as was got in LPA. The phase space is presented in Fig. 12. The point $z_c^* = 1/8\pi$ and $\tilde{u}_c^* = 0$ is now called the Kosterlitz-Thouless (KT) fixed point. There is a separatrix which divides the phase space into two parts. The trajectories tending to the line of fixed points belong to the symmetric phase, all other trajectories constitute the broken phase. Around the KT point an essential scaling appears due to the infinite order phase transition in the model.

3. Exact RG equations

The RG equations can be obtained exactly when $b = 1$ in this approximation (where the potential contains only the fundamental mode, and the wavefunction renormalization is field independent). The flow equations are

$$\begin{aligned}\dot{\tilde{u}} &= -2\tilde{u} + \frac{1}{2\pi\tilde{u}z} \left[1 - \sqrt{1 - \tilde{u}^2} \right], \\ \dot{z} &= -\frac{1}{24\pi} \frac{\tilde{u}^2}{(1 - \tilde{u}^2)^{3/2}}.\end{aligned}\quad (73)$$

The phase structure is plotted in Fig. 13. One can easily see that the phase structure of the linearized treatment in Fig. 12 is a part of this phase space around the KT point. The separatrix was a straight line there which is now curved. If one tries to find the fixed points of the model then immediately realizes that it has not got any. However the phase structure suggests, that there is the line of fixed points at $\tilde{u}^* = 0$, and it seems that we have an IR fixed point in the broken phase at $\tilde{u}^* = 1$ and $1/z^* = 0$. Furthermore a UV attractive NGFP appears at $\tilde{u}^* = 1$ and $z^* = 0$. Let us see them one by one.

Line of fixed points

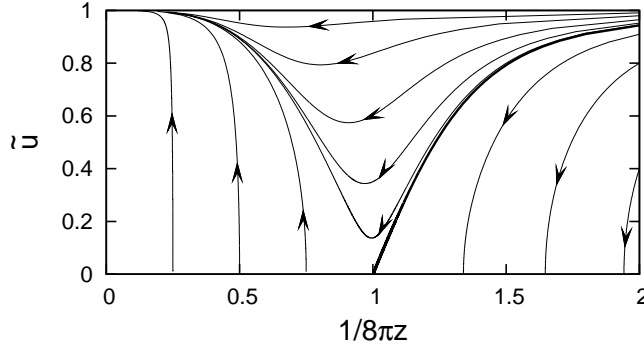


FIG. 13: The phase structure of the 2d sine-Gordon model. The separatrix is denoted by a thick line.

The line of fixed points can be found at $\tilde{u}^* = 0$ with arbitrary z^* . Its scaling behavior can be obtained by expanding the RG flow equations in Eq. (73) in \tilde{u} which gives back the approximate equations in Eq. (71). Thus we have the same scaling behavior, i.e. a relevant scaling for $z^* > 1/8\pi$ and an irrelevant one for $z^* < 1/8\pi$ and the different scaling regimes are separated by the KT point at $\tilde{u}_c^* = 0$ and $z_c^* = 1/8\pi$.

IR fixed point

The IR fixed point is situated at $\tilde{u}^* = 1$ and $1/z^* = 0$ in the broken phase. It cannot be found directly from equations in Eq. (73), too, therefore we should reparameterize the couplings. After introducing $\omega = \sqrt{1 - \tilde{u}^2}$, $\chi = 1/z\omega$ and $\partial_\tau = \omega^2 k \partial_k$ we arrive at the evolution equations

$$\begin{aligned}\partial_\tau \omega &= 2\omega(1 - \omega^2) - \frac{\omega^2 \chi}{2\pi}(1 - \omega), \\ \partial_\tau \chi &= \chi^2 \frac{1 - \omega^2}{24\pi} - 2\chi(1 - \omega^2) + \frac{\omega \chi^2}{2\pi}(1 - \omega),\end{aligned}\quad (74)$$

possessing the fixed point $\omega^* = 0$ and arbitrary χ^* which corresponds to $\tilde{u}^* = 0$ and arbitrary z^* , thus we get back the lines of fixed points. However there is another fixed point at $\chi^* = 0$ and $\omega^* = 0$, which can be identified by the IR fixed point at $1/z^* = 0$ and $\tilde{u}^* = 1$, which is IR attractive.

If we introduce $\bar{k} = \min(zp^2 + R)$, the RG evolution becomes singular at $k = k_c$ when

$$\bar{k}^2 - V_k''(\phi = 0)|_{k=k_c} = 0, \quad (75)$$

where $\bar{k}^2 = bk^2[z/(b-1)]^{1-1/b}$, when $b = 1$, then $\bar{k} = k$. The solution of this equation defines the scale where the potential becomes degenerate.

The normalized coupling \bar{u} tends to 1 for every value of b . It shows that the degenerate potential (which satisfies Eq. (75)) occurs in the IR limit of the broken phase independently of the RG scheme. In the symmetric phase the evolution of z is negligible in the IR giving the same evolution as was obtained in LPA with the line of fixed points.

One can easily show that the critical exponent η_v characterizing the vortex-vortex correlation function [144] is $\eta_v = 1/4$ independently of the parameter b [28]. However the anomalous dimension for the correlation function of the field variables gives $\eta = 0$ in the vicinity of the KT point. In the deep IR scaling region the situation changes significantly, there new scaling laws appear. Fig. 14 shows that around the KT point (at about $k/\lambda \sim 10^{-4}$) z is practically constant, giving $\eta = 0$, while in the IR region z starts to diverge according to a power law scaling. This scaling regime is induced by the IR fixed point. The corresponding exponent depends on the scheme, i.e. on the value of b . The coupling \bar{u} shows the same qualitative behavior. If one plots z as the function of \bar{k} then one obtains the results of Fig. 15. The flows show sharp singularities as the function of the scale \bar{k} so as the other couplings, making the evolution scheme independent. The modes which are integrated out during the RG procedure can be indexed not only by the scale k but the scale \bar{k} and one has a smallest value of the scale \bar{k}_c . Again one can identify the correlation length according to $\xi = 1/\bar{k}_c$, furthermore the critical exponent also can be identified in a similar manner as was introduced in the d -dimensional $O(N)$ model. In the 2d SG model the temperature is proportional to z_{k_Λ} , and thus the reduced temperature t is $t \sim z_{k_\Lambda} - z_{c, k_\Lambda}$, where z_{c, k_Λ} is the initial value of the wavefunction renormalization at the separatrix. In order to demonstrate whether the phase structure is qualitatively the same we plotted it for $b = 5$ in Fig. 16. In its inset we plotted $\log \xi$ as the function of t . We obtained a straight line implying the scaling of ξ

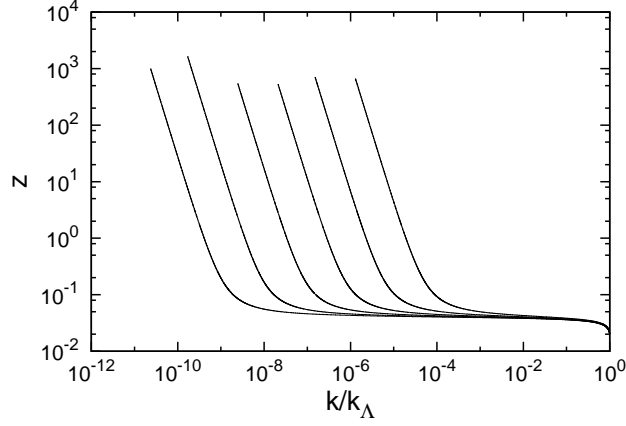


FIG. 14: The scaling of the wavefunction renormalization z is plotted as the function of k . The initial values are: $z(k_\Lambda) = 0.6$ and $\tilde{u}(k_\Lambda)$ around 1.95.

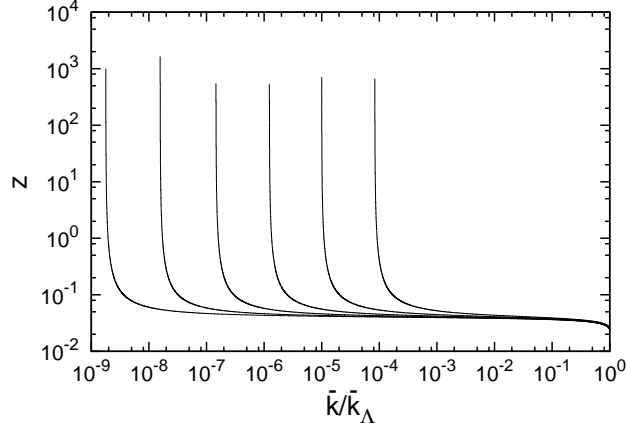


FIG. 15: The scaling of the wavefunction renormalization z is plotted as the function of \bar{k} . The initial values are: $z(k_\Lambda) = 0.6$ and $\tilde{u}(k_\Lambda)$ around 1.95.

according to

$$\log \xi \propto t^{-\nu}. \quad (76)$$

There are two types of correlation lengths, one is defined as usual, i.e. around the KT turning point of the coupling \bar{u} . Another one is identified as $\xi = 1/k_c$ in the neighborhood of the IR fixed point. It can be seen from the inset of Fig. 16 that the scaling of ξ shows an infinite order phase transition for all schemes with the exponent $\nu \approx 0.5$.

We obtained that the exponent ν coincides calculated around the KT and IR points. This is due to fact that condensate is a global object in the broken phase which is perceptible at practically any scale. The other exponents do not necessarily coincide at the KT and the IR points, e.g. the anomalous dimension $\eta = 0$ around the KT point, while it is $\eta = 2b/(b-1)$ around the IR one.

The singularity at low scales appears because the condition in Eq.(75) is satisfied. The condition shows that there are many modes in the model with infinitesimally small, practically zero energies, they are called soft modes. The ground state of the model can pick up arbitrary number of these fluctuations, which makes the ground state degenerate. The huge amount of soft modes constitute the condensate in the broken phase. They signal that the microscopic degrees of freedom are not suitable to describe the model anymore in the broken phase at those small energy scales, one should turn to new field variables. It is reminiscent of the composition of hadrons from quarks, which are the original degrees of freedom in QCD.

One can conclude that the IR fixed point provides us the low energy limit of the theory under investigation. On the other hand the soft modes suggests that the quantum-classical transition appears in the broken phase, however

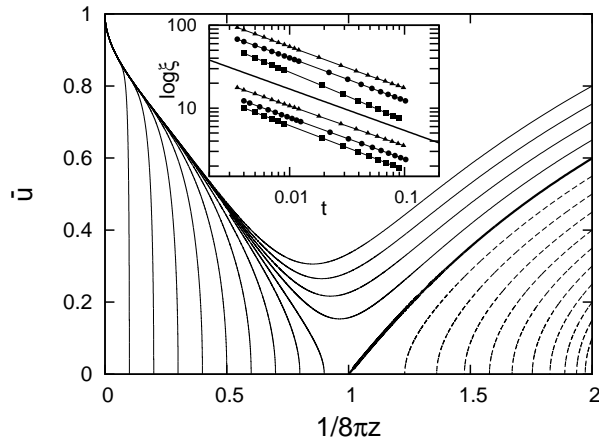


FIG. 16: Phase diagram of the SG model, with $b = 5$. The dashed (solid) lines represent the trajectories belonging to the (broken) symmetric phase, respectively. The wide line denotes the separatrix between the phases. The KT point can be considered as the crossover fixed point. The inset shows the scaling of the correlation length as the function of the reduced temperature t . The curves are shifted for better visibility. The lower (upper) set of lines corresponds to the IR (KT) fixed point. The triangle, circle and square correspond to $b = 2, 5, 10$, respectively. In the middle a straight line with the slope $-1/2$ is drawn to guide the eye.

correct treatment should be discussed by the close time path method [17, 145].

UV NGFP

The UV NGFP also cannot be seen directly analytically but it can be easily recognized in the top right corner of the phase diagram in Fig. 13. The LPA approximation trivially shows that in the UV attractive NGFP the model has a singularity, as in the IR fixed point. The UV singularity signals the upper limit of the applicability of the 2d SG model. It implies that at high energies the model requires new elementary excitations. One can make it more apparent in the framework of the XY model, which is in the same universality class as the 2d SG model. There the excitations are represented by vortices consisting of concentric forms of spins [146]. The blocking towards the higher scales means that the vortices have smaller and smaller diameter. Naturally at a certain scale we reach a limit, where the vortex reduces to a single spin. At this scale the new elementary excitations should be the single spins instead of the original vortices. Therefore in the UV limit the system of the charged vortices should be replaced by a neutral spin system.

The 2d SG model shows a nice example, where the functional RG method gives us both the high and low energy scale limits of its applicability. The low energy limit is usually indicated by the IR fixed point as was demonstrated in the article for many models. There the global interaction belonging to the condensate of the broken phase becomes IR relevant and introduces new excitations. However there should be an UV limit of the models, since it seems nonphysical to assume that a model can be valid at arbitrarily high energies. So far the functional RG method gave the upper UV limit only for the 2d SG model and its generalizations (massive [147, 148] or layered [86, 149–153] SG models).

D. Quantum Einstein gravity

The QEG is the quantum field theoretic model of gravity [93, 107]. There the metric fields are considered as fundamental degrees of freedom, and play the role of the field variable, thus the model can be treated in the framework of path integral formalism. The simplest version of the model contains the Newton constant G_k and the cosmological constant Λ_k as couplings. According to their canonical dimensions the dimensionless cosmological constant $\lambda = k^{-2}\Lambda_k$ is relevant, i.e. perturbatively renormalizable, however the dimensionless Newton constant g scales in irrelevant manner, since $g = Gk^{d-2}$. Thus the model seems to be non-renormalizable according to perturbative considerations. This might be the signal of the necessity to introduce new dynamical variables for elementary excitations, e.g. strings.

However the concept of asymptotic safety may give a helping hand to QEG. It was shown that the model has an UV attractive NGFP, which makes QEG renormalizable [78, 88, 89, 91, 96] and shows asymptotic safety [103, 104, 154–158]. It is a great challenge to find experimental evidence for quantum gravity, however there are promising ideas to

catch its effects in LHC [159, 160]. Usually the model is considered in $d = 4$, however the 3-dimensional [161] and higher dimensional cases [162–164] are also thoroughly investigated. In the context of dimension we notice that a dimensional reduction takes place during the flow to small distances from $4 \rightarrow 2$ [93, 165–167]. The bare action of QEG belongs to the UV attractive NGFP of the RG flows [93, 167]. Some kind of classical limit can be associated to any fixed points, which can give different General Relativity and cosmology [157].

QEG is defined through a diffeomorphism invariant functional of the metric $g_{\mu\nu}$ in QEG, and the background field technique is used to preserve the gauge symmetry when the RG flow equations are derived. Here we flash the main points of the derivation given in [78]. The functional integral should be performed over all metrics $\gamma_{\mu\nu}$. It is decomposed into

$$\gamma_{\mu\nu}(x) = \bar{g}_{\mu\nu}(x) + h_{\mu\nu}(x) \quad (77)$$

where $\bar{g}_{\mu\nu}(x)$ is the background field metric and $h_{\mu\nu}(x)$ is the new integration variable. The generating functional is

$$\exp\{W_k\} = \int \mathcal{D}[h_{\mu\nu}; \mathcal{C}; \bar{\mathcal{C}}] \exp\{-S[\bar{g} + h] - S_{gf}[h; \bar{g}] - S_{gh}[h, \mathcal{C}, \bar{\mathcal{C}}; \bar{g}] - \Delta_k S[h, \mathcal{C}, \bar{\mathcal{C}}; \bar{g}] - S_{source}\}, \quad (78)$$

where $S[\bar{g} + h] = S[\gamma]$ is the classical action, which is invariant under the general coordinate transformation (\mathcal{L}_v is the Lie derivative w.r.t. the vector field v)

$$\delta\gamma_{\mu\nu} = \mathcal{L}_v \equiv v^\rho \partial_\rho \gamma_{\mu\nu} + \partial_\mu v^\rho \gamma_{\rho\nu} + \partial_\nu v^\rho \gamma_{\mu\rho}. \quad (79)$$

The term S_{gf} in Eq. (78) denotes the gauge fixing term

$$S_{gf}[h; \bar{g}] = \frac{1}{2\alpha} \int d^d x \sqrt{\bar{g}} \bar{g}^{\mu\nu} F_\mu F_\nu, \quad (80)$$

where F_μ is linear in the field variable $h_{\mu\nu}$ and contains a certain form of a first order differential operator of $\bar{g}_{\mu\nu}$ [78]. The term S_{gh} stands for the Faddeev-Popov term with the ghosts C^μ and \bar{C}_μ

$$S_{gh}[h, C, \bar{C}; \bar{g}] = -\frac{1}{\kappa} \int d^d x \bar{C}_\mu \bar{g}^{\mu\nu} \frac{\partial F_\nu}{\partial h_{\alpha\beta}} \mathcal{L}_C(\bar{g}_{\alpha\beta} + h_{\alpha\beta}), \quad (81)$$

with $\kappa = (32\pi G)^{-1/2}$. It is obtained by applying the gauge transformation

$$\delta h_{\mu\nu} = \mathcal{L}_v \gamma_{\mu\nu}, \quad \delta \bar{g}_{\mu\nu} = 0 \quad (82)$$

to F_μ and then replacing the parameters v^μ by the ghost field C^μ . The Faddeev-Popov determinant is represented by the path integrals over C^μ and \bar{C}_μ . The IR regulator should be applied to both the ghost and the gravitational field, and it reads as

$$\Delta_k S[h, C, \bar{C}; \bar{g}] = \frac{1}{2} \kappa^2 \int d^d x \sqrt{\bar{g}} h_{\mu\nu} \mathcal{R}^{grav}[\bar{g}]^{\mu\nu\rho\sigma} h_{\rho\sigma} + \sqrt{2} \int d^d x \sqrt{\bar{g}} \bar{C}_\mu \mathcal{R}^{gh}[\bar{g}] C^\mu. \quad (83)$$

The source terms in Eq. (78) has the form

$$S_{source} = - \int d^d x \sqrt{\bar{g}} (t^{\mu\nu} h_{\mu\nu} + \bar{\sigma}_\mu C^\mu + \sigma^\mu \bar{C}_\mu + \beta^{\mu\nu} \mathcal{L}_C(\bar{g}_{\mu\nu} + h_{\mu\nu}) + \tau_\mu C^\nu \partial_\nu C^\mu). \quad (84)$$

In order to get the effective action one should introduce the classical field variables

$$\bar{h}_{\mu\nu} = \frac{1}{\sqrt{\bar{g}}} \frac{\delta W_k}{\delta t^{\mu\nu}}, \quad \xi_\mu = \frac{1}{\sqrt{\bar{g}}} \frac{\delta W_k}{\delta \bar{\sigma}^\mu}, \quad \bar{\xi}_\mu = \frac{1}{\sqrt{\bar{g}}} \frac{\delta W_k}{\delta \sigma^\mu}, \quad (85)$$

and then it can be obtained by the following Legendre transformation

$$\Gamma_k = \int d^d x \sqrt{\bar{g}} (t^{\mu\nu} \bar{h}_{\mu\nu} + \bar{\sigma}_\mu \xi^\mu + \sigma^\mu \bar{\xi}_\mu) - W_k + \Delta S_k. \quad (86)$$

Finally one arrives at the flow equation of the form

$$\dot{\Gamma}_k[\bar{h}, \xi, \bar{\xi}, \bar{g}] = \frac{1}{2} \text{Tr} \frac{\sqrt{2}(\dot{\mathcal{R}}_k^{grav})_{\bar{h}\bar{h}}}{(\sqrt{2}\mathcal{R}_k^{grav} + \Gamma_k'')_{\bar{h}\bar{h}}} - \frac{1}{2} \text{Tr} \left[\kappa^2 (\dot{\mathcal{R}}_k^{gh})_{\bar{\xi}\xi} \left(\frac{1}{(\kappa^2 \mathcal{R}_k^{gh} + \Gamma_k'')_{\bar{\xi}\xi}} - \frac{1}{(\kappa^2 \mathcal{R}_k^{gh} + \Gamma_k'')_{\bar{\xi}\xi}} \right) \right]. \quad (87)$$

A general form of the QEG effective action is

$$\Gamma_k = \int d^d x \sqrt{\det g_{\mu\nu}} \left(\frac{1}{16\pi G_k} (2\Lambda_k - R) - \frac{\omega_k}{3\sigma_k} R^2 + \dots + \frac{1}{2\sigma_k} C^2 + \frac{\theta_k}{\sigma_k} E + \dots + \text{gf. terms} + \text{gh. terms} \right). \quad (88)$$

The first terms come from the Taylor expansion of the general non-local functional $f(R)$ [168, 169]. The first two terms constitute the Einstein-Hilbert truncation, with the two dimensionless couplings $\lambda = \Lambda_k k^{-2}$ and $g = G_k k^{d-2}$. Then the contributions coming from the square of the Weyl tensor $C^2 = C_{\mu\nu\rho\sigma} C^{\mu\nu\rho\sigma}$, and the Gauss-Bonnet topological invariant $E = R_{\mu\nu\rho\sigma} R^{\mu\nu\rho\sigma} - 4R_{\mu\nu} R^{\mu\nu} + R^2$ are considered [170] in Eq. (88). In the end the gauge fixing and the ghost terms are indicated. The functional $f(R)$ can have any form, e.g. it can be a logarithmic or polynomial function [168]. The explicit form of the evolution equations including the interaction term R^2 can be found in [171]. A further possible extension of QEG contains terms in the action in Eq. (88) which describes interaction between the matter and the metric fields. The matter field can be a fermionic system [172–174] a scalar field [102, 175–180], or a gauge field [108, 181, 182]. The improvement of the ghost sector is also intensively studied [183, 184].

From the extensions of the QEG effective action in Eq. (88) one can derive the RG evolution equations for the couplings. Considering the 2-dimensional projection of the phase space to the usual Newton and cosmological couplings we can obtain different types of phase structures. However it has several universal properties, namely that any extension of QEG shows two phases and a possesses a UV attractive NGFP, implying that model is asymptotically safe.

E. Evolution equation

Using the Litim's regulator and the Einstein-Hilbert truncation, where the dimensionless Newton and the cosmological couplings are considered, we obtain the following RG equations [164]

$$\begin{aligned} \dot{\lambda} &= -2\lambda + \frac{g}{2} d(d+2)(d+5) - d(d+2) \frac{g}{2} \frac{(d-1)g + \frac{1-4\lambda(1-1/d)}{d-2}}{g - g_b}, \\ \dot{g} &= (d-2)g + \frac{(d+2)g^2}{g - g_b}, \end{aligned} \quad (89)$$

with

$$g_b = \frac{(1-2\lambda)^2}{2(d-2)}. \quad (90)$$

One can introduce the gravitation anomalous dimension

$$\eta = \frac{(d+2)g}{g - g_b}. \quad (91)$$

The model has two fixed points [162, 163, 185]. When $d = 4$, then there is a UV NGFP at $\lambda_{UV}^* = 1/4$, $g_{UV}^* = 1/64$. The matrix M is

$$M = \frac{1}{3} \begin{pmatrix} -2 & -176 \\ -1 & -8 \end{pmatrix}, \quad (92)$$

with the eigenvalues $s_{UV1} = (-5 + i\sqrt{167})/3$ and $s_{UV2} = (-5 - i\sqrt{167})/3$, so it is an UV attractive of IR repulsive focal point. Furthermore one has a GFP at $\lambda_G^* = 0$, $g_{UV}^* = 0$ with the corresponding matrix

$$M = \frac{1}{3} \begin{pmatrix} -2 & \frac{1}{2}d(d+2)(d-3) \\ -1 & d-2 \end{pmatrix} \quad (93)$$

in dimension d . The eigenvalues are $s_{G1} = -2$ and $s_{G2} = d-2$. The negative reciprocal of the former eigenvalue gives the critical exponent $\nu = 1/2$ of ξ . The latter one guarantees that the GFP is a hyperbolic one when $d > 2$.

The phase structure is shown in Fig. 17. There is a separatrix connecting the UV attractive NGFP and the GFP. The trajectories which are left to the separatrix give negative values for the cosmological constant and vanishing Newton coupling in the IR limit, and constitute the strong-coupling or symmetric phase of QEG [78, 186]. Other

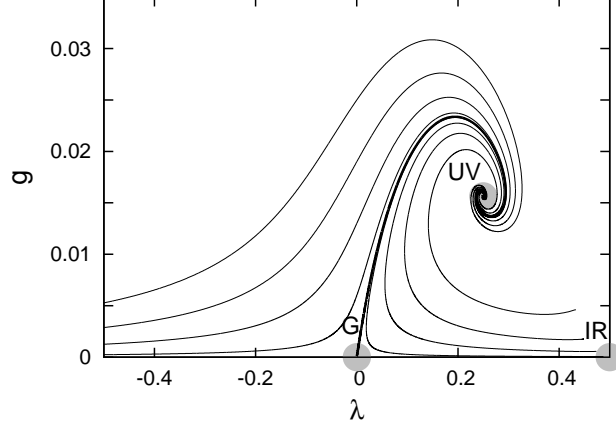


FIG. 17: The phase structure of quantum Einstein gravity in $d = 4$ is shown. There is an UV attractive NGFP, a crossover fixed point, which is now the Gaussian one, and an IR fixed point. The thick line represents the separatrix.

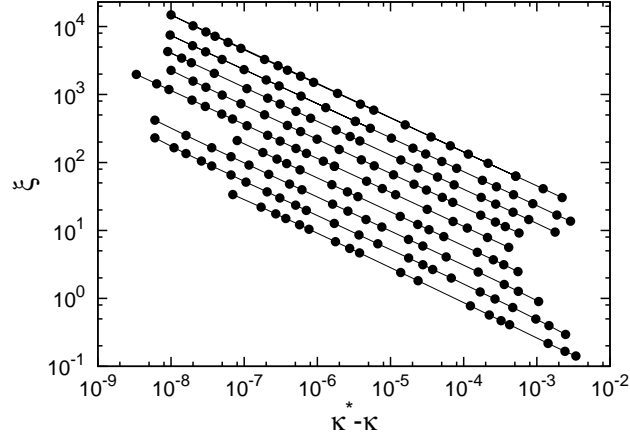


FIG. 18: The scaling of the correlation length, giving $\nu = 1/2$ for the exponent. For simplicity we fixed the UV value of g_{Λ} .

trajectories getting around the separatrix from the right give large positive values of λ and small Newton coupling when the RG flows approach the IR regime. This phase is called the weak-coupling or broken symmetric phase.

In $d = 4$ if one reparametrizes the couplings according to $\chi = 1 - 2\lambda$, $\omega = 4g - (1 - 2\lambda)^2$ and introduces the new 'RG time' $\partial_{\tau} = \omega \partial_t$ then one obtains

$$\begin{aligned}\partial_{\tau}\chi &= -4\omega + 2\chi\omega(8 + 21\chi) + 24\omega^2 + 6\chi^2(3\chi(\chi + 1) - 1), \\ \partial_{\tau}\omega &= 8\omega^2(1 - 6\chi) - 2\chi(42\chi^2 + 9\chi - 4) - 6\chi^3(\chi(6\chi + 5) - 2),\end{aligned}\tag{94}$$

which have the UV NGFP at $\omega_{UV}^* = -3/16$ and $\chi_{UV}^* = 1/2$, the GFP at $\omega_G^* = -1$ and $\chi_G^* = 1$ and the IR attractive fixed point at $\omega_{IR}^* = 0$ and $\chi_{IR}^* = 0$ which corresponds to the point $g_{IR}^* = 0$ and $\lambda_{IR}^* = 1/2$ in terms of the original dimensionless couplings. Naturally the IR fixed point is IR attractive. The existence of the IR fixed point also has been uncovered and discussed in [108–110].

As in the case of the previous models, one can get the value of the critical exponent ν from the IR scaling. Again, the scale k where the evolution stops equals the reciprocal of the correlation length ξ . We plotted the divergence of the correlation length in Fig.18 for dimensions $d = 4 \dots 11$. We obtain that a second order phase transition can be identified in the IR region of QED with the exponent $\nu = 1/2$ independently on the dimension. One can obtain similar results if one uses different regularization scheme or special extensions of the action containing the functions of the Euclidean spacetime volume $V = \int d^d x \sqrt{\det g_{\mu\nu}}$ [87]. This result does not coincide to the UV value of $\nu = 1/3$ [187, 188], which is the reciprocal of the imaginary part of the scaling exponent in the UV fixed point, i.e. $\nu = 3/\sqrt{167} \approx 0.23$. They are not equal but taking into account further couplings e.g. by including higher order

model	UV	CO	IR
3d $O(N)$ model	Gaussian	Wilson-Fisher	IR
3d nonlinear σ model	non-Gaussian	non-Gaussian	Gaussian
3d Gross-Neveu model	Gaussian	non-Gaussian	IR
2d sine-Gordon model	Gaussian and non-Gaussian	Kosterlitz-Thouless	Gaussian and IR
4d quantum Einstein gravity	non-Gaussian	Gaussian	IR

TABLE III: Summary of the models and their fixed points.

terms in the curvature scalar [118, 189–194] the result of ν can be improved. Generally the exponent has some scheme and truncation dependence, and it is around $\nu \approx 0.23 - 0.4$.

However the improvement of the action by extensions does not necessarily change the IR value of $\nu = 1/2$. As it was demonstrated through many models in the previous sections the IR value of ν equals the one which can be calculated in the vicinity of the crossover hyperbolic fixed point if it exists. Here the GFP plays this role, but we know that the eigenvalues of the GFP equals the negative canonical dimension of the couplings. The single negative eigenvalue of M in Eq. (93) is $s_1 = -2$ independently on the dimension, as is numerically checked and shown in Fig. 18. If we introduce new couplings into the QEG effective action in Eq. (88) as a Taylor expansion of the dimensionless form of $\tilde{f}(\tilde{R})$ [195] according to

$$\tilde{f}(\tilde{R}) = \sum_{n=1}^N \frac{\tilde{g}_n}{n!} \tilde{R}^n, \quad (95)$$

then the canonical dimension of the coupling \tilde{g}_n becomes $d_n = d - 2n$. We can identify the first two dimensionless couplings with the cosmological and the Newton couplings as $\lambda \sim \tilde{g}_0/\tilde{g}_1$ and $g \sim 1/\tilde{g}_1$. Then the canonical dimension induced scaling of the couplings around the GFP are $\lambda \sim k^{-2}$, $g \sim k^{d-2}$ and $\tilde{g}_n \sim k^{2n-d}$ with $n > 1$. In case of $d = 4$ the single negative eigenvalue is $s_1 = -2$, which belongs to the cosmological coupling. It implies that the exponent ν calculated at the GFP is always equals $1/2$, therefore we expect, that its IR value is exactly $\nu = 1/2$ if the total $\tilde{f}(\tilde{R})$ is considered.

We note that there are extensions of QEG where the GFP does not exist [107]. Since the IR fixed point is strongly related to the crossover hyperbolic point then its scaling behavior can significantly change. It was shown that a certain choice of the extension may eliminate the GFP [87]. In this case the correlation length ξ does not diverge which implies that the order of the phase transition changes to a first order one, in the IR region. Naturally it can also change the classical limit there which may also affect the cosmological value problem [87].

IV. SUMMARY

We gave a short introduction of asymptotic safety in the framework of the functional renormalization group method. We introduced several models, where a nontrivial UV attractive fixed point exists, which saves the model from nonphysical divergences and gives asymptotic safety.

The functional renormalization group method is a powerful nonperturbative tool to investigate the field theoretical models. It provides a partial differential equation for the effective action which initial condition describes the high energy UV physics of the model and the solution gives the low energy IR one. The RG technique is used in several areas in quantum physics, however the results from its nonperturbative nature comes forward quite rarely. One can say that the stable UV and the stable IR limit of the theory cannot be described by perturbative calculations. The former one provides the asymptotic safety, while the latter one gives the IR behavior of the broken phase which can be related to the quantum-classical transition. In this articles we concentrated on these limits of the models which were considered.

First we investigated the d -dimensional $O(N)$ model, which is asymptotically free. We showed that there exists two phases and three fixed points in the model. Then we analyzed such models which are asymptotically safe. We plotted the phase structure of the 3d nonlinear σ , the 3d Gross-Neveu, the 2d sine-Gordon models and the 4d quantum Einstein gravity. These models have two phases. The phase space shows several similarities. There are three different fixed points. The trajectories start from the UV attractive NGFP and tend towards the crossover hyperbolic fixed point. In the broken phase of the models there exists a further IR fixed point which is IR attractive. Table III summarizes the fixed points of the models, which were investigated. The models are not in the same universality class, since they

can be distinguished by the critical exponents. Different fixed points may result in different exponents, therefore the classification could be done for the UV, CO and the IR fixed points.

Acknowledgments

The work is supported by the project TÁMOP 4.2.1./B-09/1/KONV-2010-0007. The project is implemented through the New Hungary Development Plan co-financed by the European Social Fund, and the European Regional Development Fund.

-
- [1] C. Wetterich, Phys.Lett. **B301**, 90 (1993).
 - [2] J. Berges, N. Tetradis, and C. Wetterich, Phys.Rept. **363**, 223 (2002), hep-ph/0005122.
 - [3] J. Polonyi, Central Eur.J.Phys. **1**, 1 (2003), hep-th/0110026.
 - [4] J. M. Pawłowski, Annals Phys. **322**, 2831 (2007), hep-th/0512261.
 - [5] H. Gies (2006), hep-ph/0611146.
 - [6] B. Delamotte (2007), cond-mat/0702365.
 - [7] O. J. Rosten, Phys.Rept. **511**, 177 (2012), 1003.1366.
 - [8] A. Horikoshi, K.-I. Aoki, M.-a. Taniguchi, and H. Terao, pp. 194–203 (1998), hep-th/9812050.
 - [9] A. Kapoyannis and N. Tetradis, Phys.Lett. **A276**, 225 (2000), hep-th/0010180.
 - [10] D. Zappala, Phys.Lett. **A290**, 35 (2001), quant-ph/0108019.
 - [11] K.-I. Aoki, A. Horikoshi, M. Taniguchi, and H. Terao, Progress of Theoretical Physics **108**, 571 (2002), arXiv:quant-ph/0208173.
 - [12] S. Nagy and K. Sailer, Annals Phys. **326**, 1839 (2011), 1009.4041.
 - [13] K.-I. Aoki, A. Horikoshi, and E. Nakamura, Phys.Rev. **A62**, 22101 (2000), quant-ph/9912109.
 - [14] K.-I. Aoki and A. Horikoshi, Phys.Rev. **A66**, 042105 (2002), quant-ph/0205002.
 - [15] K.-I. Aoki and A. Horikoshi, Phys.Lett. **A314**, 177 (2003), quant-ph/0204078.
 - [16] S. Nagy, J. Polonyi, and K. Sailer, Acta Physica et Chimica Debrecina **XL**, 67 (2006).
 - [17] J. Polonyi, Phys.Rev. **D84**, 105021 (2011), 1109.2228.
 - [18] K.-I. Aoki and T. Kobayashi, ArXiv e-prints (2012), 1209.5827.
 - [19] S. Diehl and C. Wetterich, Phys.Rev. **A73**, 033615 (2006), cond-mat/0502534.
 - [20] S. Diehl, H. Gies, J. Pawłowski, and C. Wetterich, Phys.Rev. **A76**, 021602 (2007), cond-mat/0701198.
 - [21] W. Metzner, M. Salmhofer, C. Honerkamp, V. Meden, and K. Schonhammer, Rev.Mod.Phys. **84**, 299 (2012), 1105.5289.
 - [22] V. L. Berezinskii, Sov. Phys.-JETP **34**, 610 (1972).
 - [23] J. Kosterlitz and D. Thouless, J.Phys. **C6**, 1181 (1973).
 - [24] M. Grater and C. Wetterich, Phys.Rev.Lett. **75**, 378 (1995), hep-ph/9409459.
 - [25] G. Von Gersdorff and C. Wetterich, Phys.Rev. **B64**, 054513 (2001), hep-th/0008114.
 - [26] D. J. Amit, Y. Y. Goldschmidt, and G. Grinstein, J.Phys. **A13**, 585 (1980).
 - [27] J. Balog and A. Hegedus, J.Phys. **A33**, 6543 (2000), hep-th/0003258.
 - [28] S. Nagy, I. Nandori, J. Polonyi, and K. Sailer, Phys.Rev.Lett. **102**, 241603 (2009), 0904.3689.
 - [29] S. Nagy and K. Sailer (2010), 1012.3007.
 - [30] D. B. Kaplan, J.-W. Lee, D. T. Son, and M. A. Stephanov, Phys.Rev. **D80**, 125005 (2009), 0905.4752.
 - [31] J. Braun, C. S. Fischer, and H. Gies, Phys.Rev. **D84**, 034045 (2011), 1012.4279.
 - [32] N. Tetradis and C. Wetterich, Nucl.Phys. **B422**, 541 (1994), hep-ph/9308214.
 - [33] S.-B. Liao, J. Polonyi, and M. Strickland, Nucl.Phys. **B567**, 493 (2000), hep-th/9905206.
 - [34] D. F. Litim, Phys.Rev. **D64**, 105007 (2001), hep-th/0103195.
 - [35] R. Guida and J. Zinn-Justin, Nucl.Phys. **B489**, 626 (1997), hep-th/9610223.
 - [36] R. Guida and J. Zinn-Justin, J.Phys. **A31**, 8103 (1998), cond-mat/9803240.
 - [37] J. Zinn-Justin, Phys.Rept. **344**, 159 (2001), hep-th/0002136.
 - [38] T. R. Morris, Nucl.Phys. **B495**, 477 (1997), hep-th/9612117.
 - [39] T. R. Morris and M. D. Turner, Nucl.Phys. **B509**, 637 (1998), hep-th/9704202.
 - [40] D. F. Litim and D. Zappala, Phys.Rev. **D83**, 085009 (2011), 1009.1948.
 - [41] L. Canet, B. Delamotte, D. Mouhanna, and J. Vidal, Phys.Rev. **D67**, 065004 (2003), hep-th/0211055.
 - [42] L. Canet, B. Delamotte, D. Mouhanna, and J. Vidal, Phys.Rev. **B68**, 064421 (2003), hep-th/0302227.
 - [43] C. Bervillier, J.Phys.Condens.Matter **17**, S1929 (2005), hep-th/0501087.
 - [44] V. Pangon, S. Nagy, J. Polonyi, and K. Sailer, Int.J.Mod.Phys. **A26**, 1327 (2011), 0907.0144.
 - [45] V. Pangon, PhD thesis (2009).
 - [46] D. F. Litim, M. C. Mastaler, F. Synatschke-Czerwonka, and A. Wipf, Phys.Rev. **D84**, 125009 (2011), 1107.3011.
 - [47] M. Heilmann, D. F. Litim, F. Synatschke-Czerwonka, and A. Wipf (2012), 1208.5389.
 - [48] S. Nagy (2012), 1201.1625.

- [49] F. Benitez, R. M. Galain, and N. Wschebor, Phys.Rev. **B77**, 024431 (2008), 0708.0238.
- [50] F. Benitez, J.-P. Blaizot, H. Chate, B. Delamotte, R. Mendez-Galain, et al., Phys.Rev. **E80**, 030103 (2009), 0901.0128.
- [51] F. Benitez, J.-P. Blaizot, H. Chate, B. Delamotte, R. Mendez-Galain, et al., Phys.Rev. **E85**, 026707 (2012), 1110.2665.
- [52] P. Castorina, M. Mazza, and D. Zappala, Phys.Lett. **B567**, 31 (2003), hep-th/0305162.
- [53] J. Braun, J.Phys. **G39**, 033001 (2012), 1108.4449.
- [54] D. D. Scherer and H. Gies, Phys.Rev. **B85**, 195417 (2012), 1201.3746.
- [55] H. Gies and L. Janssen, Phys.Rev. **D82**, 085018 (2010), 1006.3747.
- [56] L. Janssen and H. Gies (2012), 1208.3327.
- [57] J. Alexandre, J. Polonyi, and K. Sailer, Phys.Lett. **B531**, 316 (2002), hep-th/0111152.
- [58] H. Gies and J. Jaeckel, Phys.Rev.Lett. **93**, 110405 (2004), hep-ph/0405183.
- [59] S. Arnone, T. R. Morris, and O. J. Rosten, JHEP **0510**, 115 (2005), hep-th/0505169.
- [60] D. F. Litim and J. M. Pawłowski, Phys.Lett. **B435**, 181 (1998), hep-th/9802064.
- [61] M. D'Attanasio and T. R. Morris, Phys.Lett. **B378**, 213 (1996), hep-th/9602156.
- [62] T. R. Morris, Nucl.Phys. **B573**, 97 (2000), hep-th/9910058.
- [63] T. R. Morris, JHEP **0012**, 012 (2000), hep-th/0006064.
- [64] S. Arnone, A. Gatti, and T. R. Morris, Phys.Rev. **D67**, 085003 (2003), hep-th/0209162.
- [65] S. Arnone, T. R. Morris, and O. J. Rosten, Eur.Phys.J. **C50**, 467 (2007), hep-th/0507154.
- [66] T. R. Morris and O. J. Rosten, Phys.Rev. **D73**, 065003 (2006), hep-th/0508026.
- [67] A. Patkos, Mod. Phys. Lett. A **27**, 1250212 (2012), 1210.6490.
- [68] D. F. Litim and J. M. Pawłowski, JHEP **0209**, 049 (2002), hep-th/0203005.
- [69] J. M. Pawłowski, D. F. Litim, S. Nedelko, and L. von Smekal, Phys.Rev.Lett. **93**, 152002 (2004), hep-th/0312324.
- [70] T. R. Morris and O. J. Rosten, J.Phys. **A39**, 11657 (2006), hep-th/0606189.
- [71] J. Braun, L. M. Haas, F. Marhauser, and J. M. Pawłowski, Phys.Rev.Lett. **106**, 022002 (2011), 0908.0008.
- [72] A. Codello and R. Percacci, Phys.Lett. **B672**, 280 (2009), 0810.0715.
- [73] R. Percacci and O. Zanusso, Phys.Rev. **D81**, 065012 (2010), 0910.0851.
- [74] R. Percacci, PoS **CLAQG08**, 002 (2011), 0910.4951.
- [75] M. Fabbrichesi, R. Percacci, A. Tonero, and O. Zanusso, Phys.Rev. **D83**, 025016 (2011), 1010.0912.
- [76] R. Percacci and L. Rachwal, Phys.Lett. **B711**, 184 (2012), 1202.1101.
- [77] D. F. Litim and J. M. Pawłowski, Phys.Lett. **B546**, 279 (2002), hep-th/0208216.
- [78] M. Reuter, Phys.Rev. **D57**, 971 (1998), hep-th/9605030.
- [79] S. R. Coleman, Phys.Rev. **D11**, 2088 (1975).
- [80] I. Nandori, J. Polonyi, and K. Sailer, Phys.Rev. **D63**, 045022 (2001), hep-th/9910167.
- [81] S. Nagy, I. Nandori, J. Polonyi, and K. Sailer, Phys.Lett. **B647**, 152 (2007), hep-th/0611061.
- [82] N. Tetradis and C. Wetterich, Nucl.Phys. **B383**, 197 (1992).
- [83] J. Alexandre, V. Branchina, and J. Polonyi, Phys.Rev. **D58**, 016002 (1998), hep-th/9712147.
- [84] J. Alexandre, V. Branchina, and J. Polonyi, Phys.Lett. **B445**, 351 (1999), cond-mat/9803007.
- [85] J. Braun, H. Gies, and D. D. Scherer, Phys.Rev. **D83**, 085012 (2011), 1011.1456.
- [86] S. Nagy, Nucl.Phys. **B864**, 226 (2012), 1204.0440.
- [87] S. Nagy, J. Krizsan, and K. Sailer, JHEP **1207**, 102 (2012), 1203.6564.
- [88] O. Lauscher and M. Reuter, Class.Quant.Grav. **19**, 483 (2002), hep-th/0110021.
- [89] M. Reuter and F. Saueressig, Phys.Rev. **D65**, 065016 (2002), hep-th/0110054.
- [90] A. Ashtekar and J. Lewandowski, Class.Quant.Grav. **21**, R53 (2004), gr-qc/0404018.
- [91] M. Reuter and F. Saueressig (2007), 0708.1317.
- [92] C. Kiefer, *Quantum Gravity*, International Series of Monographs on Physics (OUP Oxford, 2007), ISBN 9780199212521, URL <http://books.google.hu/books?id=zLDR1qgjrw4C>.
- [93] M. Reuter and F. Saueressig, New J.Phys. **14**, 055022 (2012), 1202.2274.
- [94] G. 't Hooft and M. Veltman, Annales Poincare Phys.Theor. **A20**, 69 (1974).
- [95] M. H. Goroff and A. Sagnotti, Phys.Lett. **B160**, 81 (1985).
- [96] S. Weinberg, *Ultraviolet divergences in quantum theories of gravitation. In General Relativity: An Einstein centenary survey, ed. S. W. Hawking and W. Israel* (Cambridge University Press, 1979).
- [97] S. Weinberg (1996), hep-th/9702027.
- [98] S. Weinberg (2009), 0903.0568.
- [99] S. Weinberg, PoS **CD09**, 001 (2009), 0908.1964.
- [100] S. Christensen and M. Duff, Phys.Lett. **B79**, 213 (1978).
- [101] R. Gastmans, R. Kallosh, and C. Truffin, Nucl.Phys. **B133**, 417 (1978).
- [102] R. Percacci and D. Perini, Phys.Rev. **D68**, 044018 (2003), hep-th/0304222.
- [103] R. Percacci (2007), 0709.3851.
- [104] M. Niedermaier, Class.Quant.Grav. **24**, R171 (2007), gr-qc/0610018.
- [105] M. Niedermaier and M. Reuter, Living Rev.Rel. **9**, 5 (2006).
- [106] A. Bonanno and M. Reuter, Phys.Lett. **B527**, 9 (2002), astro-ph/0106468.
- [107] M. Reuter and F. Saueressig, Phys.Rev. **D66**, 125001 (2002), hep-th/0206145.
- [108] I. Donkin and J. M. Pawłowski (2012), 1203.4207.
- [109] D. Litim, A. Satz, and A. Satz (2012), 1205.4218.
- [110] N. Christiansen, D. F. Litim, J. M. Pawłowski, and A. Rodigast (2012), 1209.4038.

- [111] H. Kleinert, *Path Integrals in Quantum Mechanics, Statistics, Polymer Physics, and Financial Markets*, International Series of Monographs on Physics (World Scientific, 2004), ISBN 981-238-106-6, URL <http://books.google.hu/books?id=zLDRlqgjrW4C>.
- [112] F. J. Wegner and A. Houghton, *Phys.Rev.* **A8**, 401 (1973).
- [113] J. Alexandre and J. Polonyi, *Annals Phys.* **288**, 37 (2001), hep-th/0010128.
- [114] C. Wetterich, *Nucl.Phys.* **B352**, 529 (1991).
- [115] K. G. Wilson, *Rev.Mod.Phys.* **47**, 773 (1975).
- [116] J. Polchinski, *Nucl.Phys.* **B231**, 269 (1984).
- [117] D. F. Litim, *Phys.Lett.* **B486**, 92 (2000), hep-th/0005245.
- [118] O. Lauscher and M. Reuter, *Phys.Rev.* **D66**, 025026 (2002), hep-th/0205062.
- [119] O. Lauscher and M. Reuter, *Phys.Rev.* **D65**, 025013 (2002), hep-th/0108040.
- [120] I. Nandori (2012), 1208.5021.
- [121] J. Polonyi, pp. 394–405 (2005), hep-th/0509078.
- [122] J. Polonyi, pp. 49–59 (2010), 1009.3652.
- [123] J. Alexandre, *Phys.Rev.* **D86**, 025028 (2012), 1205.1160.
- [124] J. Alexandre and A. Tsapalis (2012), 1211.0921.
- [125] D. Boyanovsky, H. de Vega, R. Holman, and J. Salgado, *Phys.Rev.* **D59**, 125009 (1999), hep-ph/9811273.
- [126] V. Pangon, S. Nagy, J. Polonyi, and K. Sailer, *Phys.Lett.* **B694**, 89 (2010), 0907.0496.
- [127] M. Gockeler, R. Horsley, V. Linke, P. E. Rakow, G. Schierholz, et al., *Phys.Rev.Lett.* **80**, 4119 (1998), hep-th/9712244.
- [128] E. Brezin and J. Zinn-Justin, *Phys.Rev.Lett.* **36**, 691 (1976).
- [129] E. Brezin, J. Zinn-Justin, and J. Le Guillou, *Phys.Rev.* **D14**, 2615 (1976).
- [130] R. Flore, A. Wipf, and O. Zanusso (2012), 1207.4499.
- [131] D. J. Gross and A. Neveu, *Phys.Rev.* **D10**, 3235 (1974).
- [132] M. Thies, *Phys.Rev.* **D69**, 067703 (2004), hep-th/0308164.
- [133] S. Hands, S. Kim, and J. B. Kogut, *Nucl.Phys.* **B442**, 364 (1995), hep-lat/9501037.
- [134] V. Schon and M. Thies, *Phys.Rev.* **D62**, 096002 (2000), hep-th/0003195.
- [135] S. Kehrein, *Phys.Rev.Lett.* **83**, 4914 (1999), cond-mat/9908048.
- [136] S. Kehrein, *Nucl.Phys.* **B592**, 512 (2001), cond-mat/0006403.
- [137] I. Nandori, U. Jentschura, K. Sailer, and G. Soff, *Phys.Rev.* **D69**, 025004 (2004), hep-th/0310114.
- [138] I. Nandori, S. Nagy, K. Sailer, and A. Trombettoni, *Phys.Rev.* **D80**, 025008 (2009), 0903.5524.
- [139] I. Nandori, S. Nagy, K. Sailer, and A. Trombettoni, *JHEP* **1009**, 069 (2010), 1007.5182.
- [140] I. Nandori, J. Polonyi, and K. Sailer, *Phil.Mag.* **B81**, 1615 (2001), hep-th/0012208.
- [141] I. Nandori, K. Sailer, U. Jentschura, and G. Soff, *J.Phys.* **G28**, 607 (2002), hep-th/0202113.
- [142] I. Nandori (2011), 1108.4643.
- [143] J. Alexandre and D. Tanner, *Phys.Rev.* **D82**, 125035 (2010), 1003.6049.
- [144] J. Kosterlitz, *J.Phys.* **7**, 1046 (1974).
- [145] J. Polonyi (2012), 1210.2887.
- [146] K. Huang and J. Polonyi, *Int.J.Mod.Phys.* **A6**, 409 (1991).
- [147] S. Nagy, I. Nandori, J. Polonyi, and K. Sailer, *Phys.Rev.* **D77**, 025026 (2008), hep-th/0611216.
- [148] I. Nandori, *Phys.Rev.* **D84**, 065024 (2011), 1008.2934.
- [149] I. Nandori and K. Sailer, *Phil.Mag.* **86**, 2033 (2006), hep-th/0508033.
- [150] I. Nandori, S. Nagy, K. Sailer, and U. Jentschura, *Nucl.Phys.* **B725**, 467 (2005), hep-th/0509100.
- [151] U. Jentschura, I. Nandori, and J. Zinn-Justin, *Annals Phys.* **321**, 2647 (2006), hep-th/0509186.
- [152] I. Nandori, *J.Phys.* **A39**, 8119 (2006), hep-th/0602202.
- [153] I. Nandori, *Phys.Lett.* **B662**, 302 (2008), 0707.2745.
- [154] O. Lauscher and M. Reuter, *Int.J.Mod.Phys.* **A17**, 993 (2002), hep-th/0112089.
- [155] R. Percacci (2011), 1110.6389.
- [156] A. Nink and M. Reuter (2012), 1208.0031.
- [157] A. Bonanno, *Phys.Rev.* **D85**, 081503 (2012), 1203.1962.
- [158] U. Harst and M. Reuter, *JHEP* **1205**, 005 (2012), 1203.2158.
- [159] B. Dobrich and A. Eichhorn, *JHEP* **1206**, 156 (2012), 1203.6366.
- [160] A. Eichhorn (2012), 1210.1528.
- [161] M. Demmel, F. Saueressig, and O. Zanusso (2012), 1208.2038.
- [162] D. F. Litim, *Phys.Rev.Lett.* **92**, 201301 (2004), hep-th/0312114.
- [163] P. Fischer and D. F. Litim, *Phys.Lett.* **B638**, 497 (2006), hep-th/0602203.
- [164] D. F. Litim (2008), 0810.3675.
- [165] M. Reuter and F. Saueressig, *JHEP* **1112**, 012 (2011), 1110.5224.
- [166] G. Calcagni, *Phys.Rev.* **D86**, 044021 (2012), 1204.2550.
- [167] M. Reuter and F. Saueressig (2012), 1205.5431.
- [168] P. F. Machado and F. Saueressig, *Phys.Rev.* **D77**, 124045 (2008), 0712.0445.
- [169] J. A. Dietz and T. R. Morris (2012), 1211.0955.
- [170] D. Benedetti, P. F. Machado, and F. Saueressig (2009), 0909.3265.
- [171] S. Rechenberger and F. Saueressig, *Phys.Rev.* **D86**, 024018 (2012), 1206.0657.
- [172] A. Eichhorn and H. Gies, *New J.Phys.* **13**, 125012 (2011), 1104.5366.

- [173] A. Eichhorn, J.Phys.Conf.Ser. **360**, 012057 (2012), 1109.3784.
- [174] P. Dona and R. Percacci (2012), 1209.3649.
- [175] R. Percacci and D. Perini, Phys.Rev. **D67**, 081503 (2003), hep-th/0207033.
- [176] O. Zanusso, L. Zambelli, G. Vacca, and R. Percacci, Phys.Lett. **B689**, 90 (2010), 0904.0938.
- [177] E. Manrique, M. Reuter, and F. Saueressig, Annals Phys. **326**, 440 (2011), 1003.5129.
- [178] E. Manrique, M. Reuter, and F. Saueressig, Annals Phys. **326**, 463 (2011), 1006.0099.
- [179] G. Vacca and O. Zanusso, Phys.Rev.Lett. **105**, 231601 (2010), 1009.1735.
- [180] A. Eichhorn (2012), 1204.0965.
- [181] S. Folkerts, D. F. Litim, and J. M. Pawłowski, Phys.Lett. **B709**, 234 (2012), 1101.5552.
- [182] A. Eichhorn (2011), 1111.1237.
- [183] K. Groh and F. Saueressig, J.Phys. **A43**, 365403 (2010), 1001.5032.
- [184] A. Eichhorn and H. Gies, Phys.Rev. **D81**, 104010 (2010), 1001.5033.
- [185] D. F. Litim, AIP Conf.Proc. **841**, 322 (2006), hep-th/0606044.
- [186] J. Polonyi and E. Regos, Class.Quant.Grav. **23**, 207 (2006), hep-th/0404185.
- [187] H. W. Hamber, Phys.Rev. **D45**, 507 (1992).
- [188] H. W. Hamber, Phys.Rev. **D61**, 124008 (2000), hep-th/9912246.
- [189] A. Codello and R. Percacci, Phys.Rev.Lett. **97**, 221301 (2006), hep-th/0607128.
- [190] P. Fischer and D. F. Litim, AIP Conf.Proc. **861**, 336 (2006), hep-th/0606135.
- [191] A. Codello, R. Percacci, and C. Rahmede, Int.J.Mod.Phys. **A23**, 143 (2008), 0705.1769.
- [192] D. Benedetti, K. Groh, P. F. Machado, and F. Saueressig, JHEP **1106**, 079 (2011), 1012.3081.
- [193] K. Groh, S. Rechenberger, F. Saueressig, and O. Zanusso, PoS **EPS-HEP2011**, 124 (2011), 1111.1743.
- [194] D. F. Litim, Phil.Trans.Roy.Soc.Lond. **A369**, 2759 (2011), 1102.4624.
- [195] A. Codello, R. Percacci, and C. Rahmede, Annals Phys. **324**, 414 (2009), 0805.2909.